Homeland Defense Interceptor Proposal

2005-2006 AIAA Aircraft Design Competition

Virginia Polytechnic Institute and State University

Virginia Tech

RAZERWERKS INC.

Steve Graybill
AIAA #267929
Team Leader

Zachary Kral
AIAA #267793
Materials / Structure
Configurations

Seth Taylor
AIAA #235267
Weights / Systems Avionics

Jordan Baldwin
AIAA #235268
Aerodynamics

Michael Gates
AIAA #267567
Propulsion

Nestor Urquidi
AIAA #260827
Stability & Control

Jordan Beam
AIAA #267393
Mission Performance

Alvaro Higuera
AIAA #267790
Cost Analysis

Faculty Advisor: Dr. W.H. Mason

Executive Summary

Razerwerks Inc proudly presents the *Shrike* as a solution for the 2005-2006 AIAA Undergraduate Team Aircraft Design Request for Proposal (RFP) for a Homeland Defense Interceptor aircraft (HDI). Advanced military intelligence has increased speculation that terrorist organizations have heightened activity and will presumably attack the United States from the air again. These attacks may involve large hijacked commercial airliners, small private jet aircraft, or autonomous cruise missiles. The approach for designing a multi-mission aircraft capable of providing homeland defense against possible future terrorist attacks is one that must meet all the performance requirements as well as being cost effective and easily manufactured and maintained.

The *Shrike* is a variably swept inland defense interceptor concept which utilizes maximum efficiency in both subsonic and supersonic flight regimes to reduce unnecessary fuel consumption. The aircraft's TOGW is 43,000 lbs and is considerably less than any other variable sweep aircraft. The twin engine configuration utilizes Rolls-Royce EJ200 engines that are comparatively smaller in volume yet produce a greater net thrust than larger volume single engines. Vectoring thrust provides vastly improved handling and performance that increases the maximum instantaneous turn rate as well as shortens take off distance under increased weapons loading requirements. The structure and skin of the aircraft use an Advanced Resin Transform Molding composite building process to allow more complex shapes to be easily manufactured thus reducing both weight and cost. Introduction of fly-by-light technology, incorporated with electro-hydrostatic actuation of control surfaces, has made the flight control systems lighter, highly dependable, and a quicker response time to the pilot's inputs.

The *Shrike* is capable of outperforming most tactical fighter aircraft of similar size and configuration with the use of highly advanced technology and improved materials selection, while maintaining all budgetary constraints. With a flyaway cost of $16.14 million, this multi-mission aircraft is an affordable solution to maintain a secure Nation. A comparison of the *Shrike* to other modern aircraft is shown below.

	TOGW (lbs)	Optimal Range (nm)	Max. Mach	Cost (2006 US Dollars, Million)
SHRIKE	**43000**	**4000**	**2.2**	**53.7**
F-14	72900	576	2.34	45.2
F-15	68000	3415	2.5	52.9
F-16	42300	2100	2.05	33.2
F-18	51550	2070	1.7	48.6
F-22	80000	2000	2.42	125.3

RAZERWERKS Inc,
Presents
'The Shrike'

TYPE:
A twin engine, variable sweep military interceptor, used to defend the United States homeland

WINGS:
Variable sweep to obtain optimum performance in both sub and super sonic flight

FUSELAGE:
Shaped by area ruling to obtain supersonic flight

TAILS:
Twin tail configuration with all flying horizontal tails and differential deflections

LANDING GEAR:
Tricycle landing gear minimizing components and movement involved

POWERPLANT:
Two RR EJ200 engines with thrust vectoring nozzles allowing excelling performance requirements

SYSTEMS:
Avionics – ICNIA, 3 MFDs, 8" x 20" HUD, INEWS
Flight and Propulsion Control System – Vehicle Management System and FADEC
Fire Control – IRSTS and Active Array Radar
Other Systems and Equipment – OBOGS and OBIGGS, MB ACES II Ejection Seat

PAYLOAD: Can carry up to four AIM – 9M Sidewinder missiles, four AIM – 120 AMRAAM missiles, or a combination of the two types

DIMENSIONS:
Wingspan: 766.8" – 489.5"
Wing Leading Edge Angles: 18.5° - 65°
Overall Length: 725.5"
Overall Height: 112"
TOGW: 42,000 lbs

PERFORMANCE:
Cruise: Mach 0.8 at 40,000ft
Maximum Speed: Mach 2.2
Loiter Time: 4 hours
Instantaneous Turn Rate: 18°/sec

DRAWING TITLE: THE SHRIKE
DESIGNED BY: RAZERWERKS INC
DRAFTED BY: ZACHARY KRAL

TABLE OF CONTENTS

INDEX OF TABLES

INDEX OF FIGURES

List of Variables and Abbreviations

Variables	Definition	Units
A_i	Area at station i	ft^2
a_0	Speed of sound	ft/s^2
AR	Aspect Ratio	
AR_{sub}	Subsonic Aspect Ratio	
AR_{int}	Intermediate Aspect Ratio	
AR_{sup}	Supersonic Aspect Ratio	
B	Wing span	ft
C_D	Cost of development support;	$
C_D	Drag coefficient	
C_E	Cost of airframe engineering hours	$
C_{EN}	Cost of engines	$
C_L	Lift coefficient	
$C_{L\alpha}$	3-D lift curve slope	
C_{Lmax}	Maximum lift coefficient	
C_{lmax}	Maximum section lift coefficient	
C_{LTO}	Lift coefficient for take-off	
C_{ML}	Cost of labor	$
C_{MM}	Cost of manufacturing materials	$
C_{nr}	Yaw moment due to rudder deflection	1/rad
C_{nb}	Yaw moment due to sideslip angle	1/rad
C_P	Cost of profit; Pressure coefficient	$;-
C_{QC}	Cost of quality control	$
C_T	Cost of tooling	$
D	Drag	lbs
F	Uninstalled thrust	lb
g_c	Newton constant	$lbm\text{-}ft/(lbf\text{-}s^2)$
K_i	Gain values	
$(L/D)_{max}$	Maximum lift over drag ratio	
m_0	Mass flow	lbm/s
MAC	Mean-aerodynamic chord	ft
M_i	Mach number at station i	
n_{max}	Maximum load factor	g
P_i	Pressure at station i	psi
P_s	Specific Excess Power	ft/s
P_{ti}	Total pressure at station i	psi
Q	Number of production aircraft	
S	Wing area	ft^2
T	Installed thrust	lbs
t/c	Thickness ratio	
T_i	Temperature at station i	°R
TOGW	Take-off gross weight	lbs
T_r	Period	s
TSFC	Thrust specific fuel consumption	1/hr
V	Velocity	ft/s
V_D	Wind dive velocity	ft/s

List of Variables and Abbreviations

Variables	Definition	Units
V_g	Wind gust velocity	ft/s
W	Weight	Lbs
Greek Letters	**Definition**	**Units**
Λ_{LE}	Leading edge sweep angle	°
Λ_{TE}	Trailing edge sweep angle	°
A	Angle of attack	°
Γ	Ratio of specific heats	
Z	Short period damping ratio	
ζ_{dr}	Dutch roll damping ratio	
ζ_{p}	Phugoid damping ratio	
Λ	Taper Ratio	
φ_{inlet}	Inlet installation losses	
Φ_{nozzle}	Nozzle installation losses	
ω_{sp}	Natural frequency	rad/s
ω_{ndr}	Dutch roll natural frequency	rad/s

Abbrev.	Definition
AIAA	American Institute of Aeronautics and Astronautics
AIM	Air Intercept Missile
Alt	Altitude
AMRAAM	Advanced Medium-Range Air-to-Air Missile
AOA	Angle of Attack
APU	Auxiliary Power Unit
CG	Center of Gravity
DCAP	Defensive Counter Air Patrol
EHA	Electro Hydrostatic Actuator
EM	Escort Mission
FADEC	Full Authority Digital Engineering Control
FBL	Fly by Light
FBW	Fly by Wire
HDI	Homeland Defense Interceptor
HUD	Heads-Up Display
ICNIA	Integrated Communication, Navigation, and Identification Avionics
IDG	Integrated Drive Generator
I/E	Intercept/Escort
IFF	Identify Friend or Foe
INEWS	Integrated Electronic Warfare System
IPCS	Ice Protection Control System
IRSTS	Infrared Search and Track System with laser ranging
NACA	National Advisory Committee for Aerodynamics
Nm	Nautical Mile
O&M	Operation and Maintenance
OBIGGS	On-Board Inert Gas Generation System
OBOGS	On-Board Oxygen Generation System
PBW	Power by Wire
PS	Power Setting
RDT&E	Research Development Test and Evaluation
RFP	Request for Proposal

Abbrev.	Definition
RR	Rolls Royce
RTM	Resin Transfer Molding
PDI	Point Defense Interceptor
SAS	Stability Augmentation System
SM	Static Margin
TO	Take-Off
TOGW	Take-Off Gross Weight
TOP	Take-Off Parameter
UCAV	Unmanned Combat Arial Vehicle
VMS	Vehicle Management System
WSM	Wing Sweeping Mechanism

Introduction

In response to the AIAA HDI undergraduate design project RFP, Razerwerks Inc. presents the Shrike interceptor to meet the selected mission requirements without the use of external fuel tanks or air-to-air refueling. To meet the mission criteria, several concepts were discussed and evaluated. However, variable sweep most efficiently met the requirements outlined by the RFP.

Lanius Excubitor is the Latin nomenclature for the Great Grey Shrike for which our aircraft is so appropriately named. When the Shrike seizes its prey it will fiercely peck it until it becomes subdued, thereafter it will find a sharp thorn or a barbed wire fence and impale it until dead. This advanced method of killing has dubbed the name “Butcher Bird” where Lanius is Latin for 'butcher,' and excubitor is Latin for 'watchman' or 'sentinel'. Because of its hawk like characteristics of perching and waiting for its prey, then swooping down to attack, 'The Watchful Butcher' or *Shrike* has been adopted to describe the capabilities and intent of our Homeland Defense Interceptor aircraft.

The *Shrike’*s primary role is to serve as a defensive counter-measure to terrorist attacks from the air. Unlike previous point defense interceptors, the *Shrike* is able to remain on station for longer loiter periods to prevent a possible assault on the continental United States. This ever watchful authoritative presence maintains the security and peace of mind to America’s citizens. Additionally the *Shrike* is capable of achieving speeds in excess of Mach 2, decreasing the response time to engage possible targets, thereby increasing the range of protection. The combination of speed, maneuverability, and versatility to each mission makes the *Shrike* highly effective.

With the use of modern aviation technology Razerwerks was able to design an advanced defense interceptor which is capable of accomplishing multiple missions while maintaining affordability. This practical approach to the design process has been the essential key and main driver to the evolution of the *Shrike*.

1. Mission Performance

1.1. Critical Performance Constraints

There were two major constraints that dominated the sizing relationships used to determining the thrust-to-weight and wing loading at take-off for the Shrike. The first requirement was that there should be 700 ft/s of specific excess power at 1-*g* and sea level conditions. This requirement was additionally require at a speed of Mach 0.9. A maximum instantaneous turn rate of 18 deg/sec at 35,000 ft was the next important criteria constraining the sizing diagram. Wing loading was limited to 76 psf by the maximum instantaneous turn rate requirement while the thrust-to-weight was limited to 0.95 by the specific excess power requirement. By minimizing the thrust-to-weight at take-off, the *Shrike's* engine size could be decreased. Maximizing the wing loading creates a smaller wing where the drag due to friction is minimized. Also, a higher wing loading increase performance during the sustained load factor maneuvers. Figure 1.1 plots the two main sizing requirements as well as curves for a specific excess power of 400 ft/s at 15,000 ft and Mach 0.9, a maximum dash capability of Mach 2.2 at 35,000 ft, and take-off at 5,000 ft above sea level in 8,000 ft of runway. The requirement to land in 8,000 ft at an altitude of 5,000 ft did was less rigorous than the maximum instantaneous turn rate. An Excel worksheet containing the variables for each mission segment and the specific performance requirements used Equation 1.1 to determine and plot the wing loading and thrust-to-weight curves observed in Figure 1.1.

Equation 1.1: Sea level and take-off thrust-to-weight ratios were calculated using the equation below. β is the weight fraction per segment of the mission, α is the thrust lapse ratio specific to altitude, q is the dynamics pressure at altitude, n is the maximum load factor, W_{TO}/S is the wing loading at take-off, C_{D_0} and k_1 are aerodynamic qualities of induced drag and drag constant, respectively, M and a are mach number and speed of sound, respectively, and P_s is the specific excess power at altitude and speed.

$$\frac{T_{sl}}{W_{TO}} = \frac{\beta}{\alpha}\left\{\frac{q}{\beta}\left[\frac{C_{D0}}{W_{TO}/S} + k_1\left(\frac{n\beta}{q}\right)^2 W_{TO}/S\right] + \frac{P_s}{(M\cdot a)}\right\} \qquad \textbf{(1.1)}$$

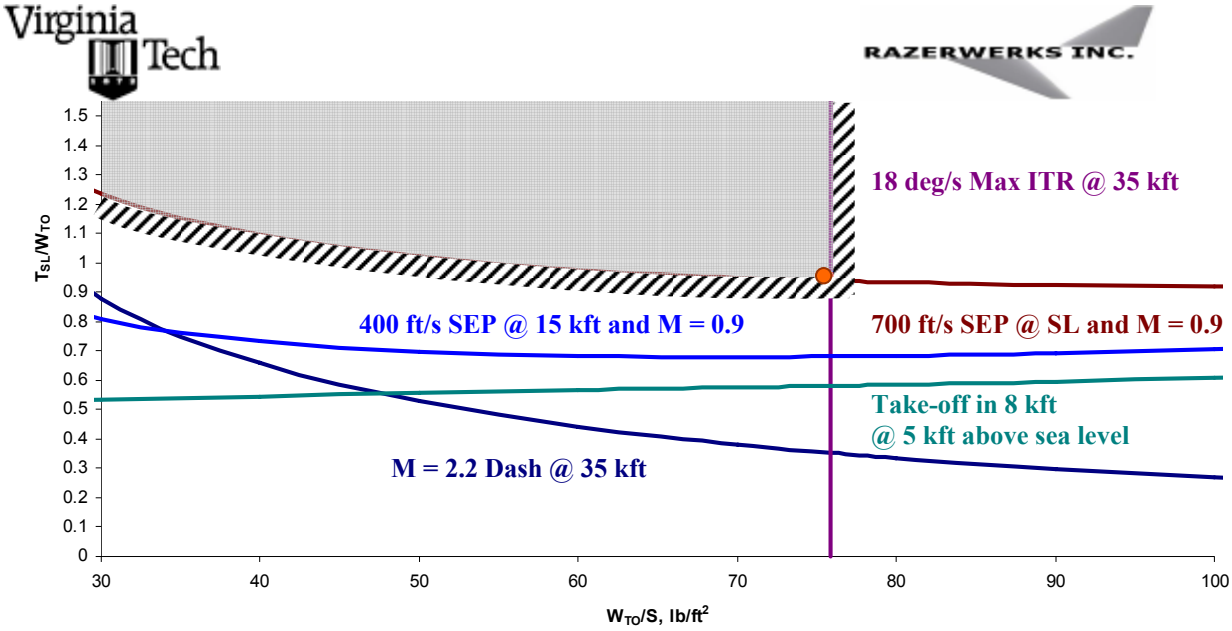

Figure 1.1: Plot of the variable sweep design's constraint curves, where the two main boundaries for the aircraft were modeled by the 18 deg/s maximum instantaneous turn rate and the 700 ft/s specific excess power curve at sea level and mach 0.9. The maximum instantaneous turn rate limited the aircraft to a wing loading at take-off of 76 psf.

Physically attaining the maximum instantaneous turn rate required a high C_{Lmax}. Unique solutions such as increasing the maximum load factor or adding vectored thrust were considered to meet this requirement. Thrust vectoring effectively increased the C_{Lmax} and raise the instantaneous turn rate to 19.5 deg/sec as seen in Figure 1.3. If the maximum load factor were increased to meet the 19.5 deg/s turn rate attained by vectored thrust the load factor would need to be increased to 8, adding 465 lbs of additional structure to the *Shrike*. Figure 1.2 and Figure 1.3 were derived using the relationships from Equation 1.2. Figure 1.2 illustrates the effects of maximizing C_L and increasing n_{max}. Designing a wing to a C_{Lmax} of 2.3 was as far as it could be pushed. Table 1.1 summarizes the cost and weight benefits between increasing n_{max} and adding vectored thrust. While the thrust vectoring is costly, it does ensure less drag during trimmed flight, enhanced maneuverability at lower speeds and decreased take-off speeds. These enhancements do not address issues in the RFP, but – while remaining under budget – will add immensely to the performance of the aircraft.

Equation 1.2: The equations below created the curves in Figure 1.2: Carpet plot of the effects of maximum lift coefficient and maximum load factor on the instantaneous turn rate versus Mach number. Increasing the load factor would allow the Shrike to perform the turn rate after the coefficient of lift had been maximized. and Figure 1.3. The instantaneous turn rate was thus affected by the maximum load factor and maximum lift coefficient.

$$M_{itr} = \frac{g\sqrt{n_{\max}{}^2 - 1}}{\omega \cdot a} \qquad \textbf{(1.2)}$$

$$\frac{W}{S} = \frac{q \cdot C_{L\max}}{n_{\max}}$$

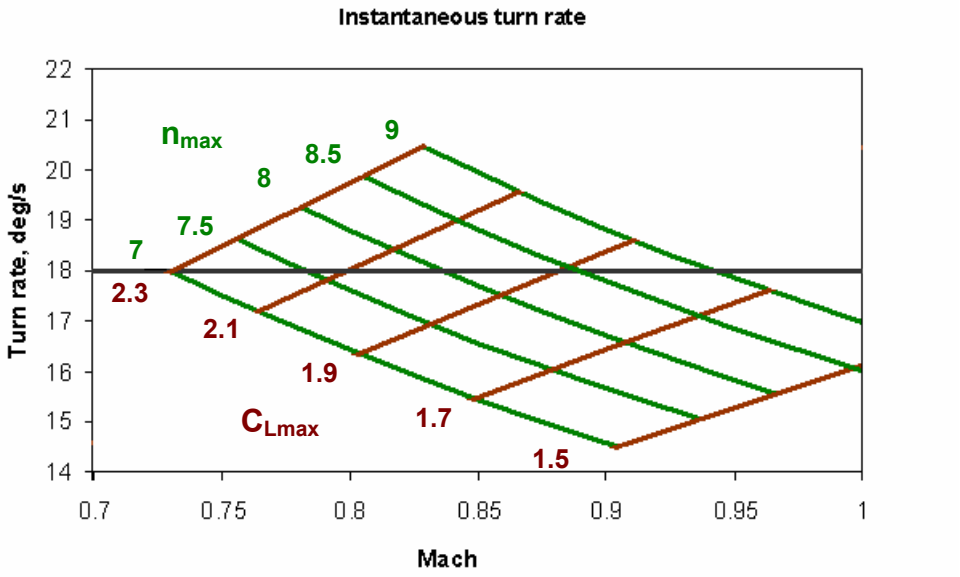

Figure 1.2: Carpet plot of the effects of maximum lift coefficient and maximum load factor on the instantaneous turn rate versus Mach number. Increasing the load factor would allow the *Shrike* to perform the turn rate after the coefficient of lift had been maximized. An acceptable load factor to secure the safety of the pilot (7) could be managed if a C_{Lmax} of 2.3 could be attained.

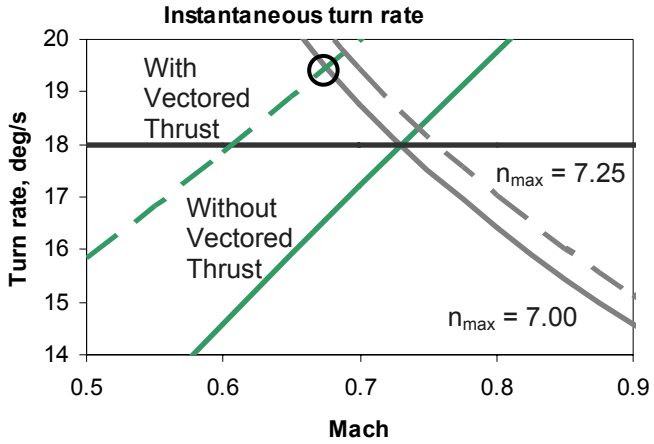

Figure 1.3: Plot showing the effects thrust vectoring has on maximum lift coefficient for the instantaneous turn rate requirement where thrust vectoring.

Table 1.1: The benefits of thrust vectoring were costly, but benefited the performance of the *Shrike* in ways simply increasing the load factor could not.

	Cost	Weight, lbs	Added Benefits
TV	$ 500,000.00	420	less drag during trimmed flight, perform ground roll without lift surfaces, improved maneuverability at lower speeds
n = 7 => n = 7.25	$ 9,420.84	119.9	aircraft withstand slightly more demanding maneuvers
n = 7 => n = 8	$ 36,547.22	465.14	aircraft withstand even more demanding maneuvers

1.2. Other Performance Constraints

In addition to the three constraints listed above, the aircraft can sustain a load factor 5 and achieve a maximum Mach of 2.2 at 35,000 ft as well as a Mach of 1.2 at sea level. A variety of specific excess power requirements include:

- 1-*g* Specific Excess Power– Military Thrust
  - 0.9M/Sea Level, P_s = 200 ft/sec
  - 0.9M/15,000 ft, P_s = 50 ft/sec
- 1-*g* Specific Excess Power– Maximum Thrust
  - **0.9M/Sea Level, P_s = 700 ft/sec***
  - 0.9M/15,000 ft, P_s = 400 ft/sec
- 5-*g* Specific Excess Power– Maximum Thrust
  - 0.9M/Sea Level, P_s = 300 ft/sec
  - 0.9M/15,000 ft, P_s = 50 ft/sec

*Bolded item indicates the most constraint sizing requirement

1.3. Missions

This aircraft will perform two missions which place vastly different constraints on the aircraft: Defensive Counter-Air Patrol and Point Defense Intercept. In addition to these missions, a third Intercept/Escort mission was used to evaluate the effective range of the aircraft while dashing, escorting and cruising. The aircraft will achieve a speed of Mach 2.2 in all missions while carrying a specified armament of two AIM-9 Sidewinders, two AIM-120 Sparrows, and a M61A1 20mm cannon with 500 rounds of ammunition. While each mission is different, the purpose of each mission is the same: Homeland Defense.

1.3.1. Defensive Counter-Air Patrol

This mission requires that stay in on station in a combat patrol for four hours. This period of loiter is substantially greater then that which can be obtained with current supersonic fighters. For example, the F-14 can only loiter for 35 minutes. A mission map can be found in Figure 1.4.

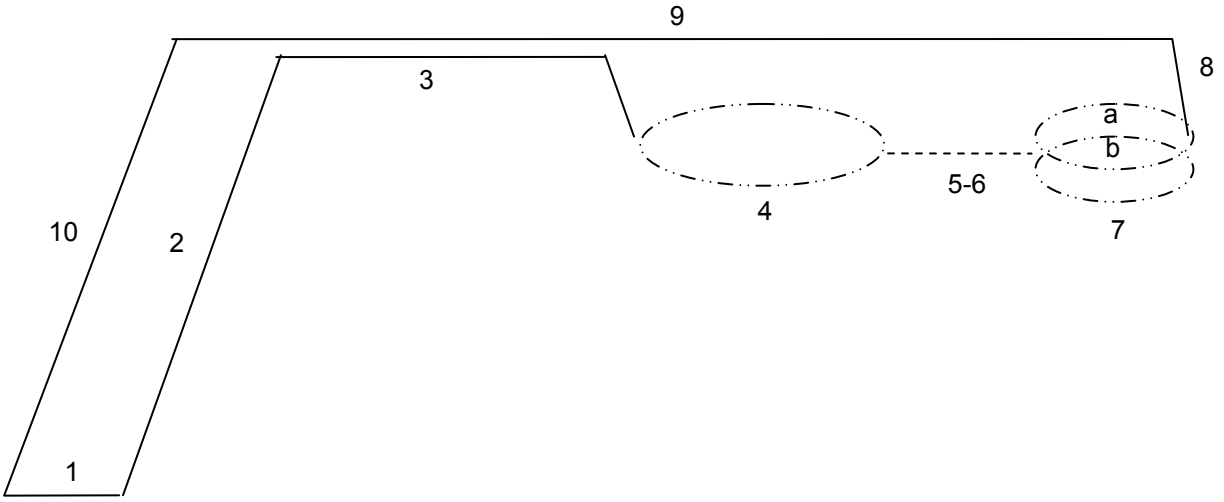

Figure 1.4: Mission Map for Defensive Counter-Air Patrol: *(1) Take off and Acceleration, (2) Climb from sea-level to optimum cruise altitude, (3) Cruise out 300 nm at optimum speed altitude, (4) Combat Air Patrol for 4 hours at best loiter speed and 35,000 ft, (5) Accelerate to maximum speed, (6) Dash 100 nm at maximum speed and 35,000 ft, (7) Combat allowance, a) One sustained 360 degree turn at mach 1.2, b) One sustained 360 degree turn at mach 0.9, (8) Climb/accelerate to optimum speed and altitude, (9) Cruise back 400 nm at optimum speed and altitude, (10) Descend to sea-level, and the final requirement which is not depicted is, Reserves for 30 minutes at speed for maximum endurance.*

The *Shrike* can complete all aspects of this mission while weighing only 42,000 lbs with 17,500 lbs of that being the fuel needed to complete all mission segments. It was determined that the best loiter speed for the design was Mach 0.8 which encompasses a vast portion of the Defensive-Counter Air Mission.

1.3.2. Point Defense Intercept Mission

This mission differs from the previous mission by having no loitering periods and longer dashing distances. The same combat maneuvers must be preformed and the same armament must be carried. Since all mission segments are essentially the same as the Defensive-Counter Air segments, the performance capabilities of this mission follow the same Mach numbers and altitudes. However, due to the lack of loiter period, the weight of fuel required drops to 5,500 lbs which increases the thrust to weight ratio to 2.6. Figure 1.5 shows a map of this particular mission.

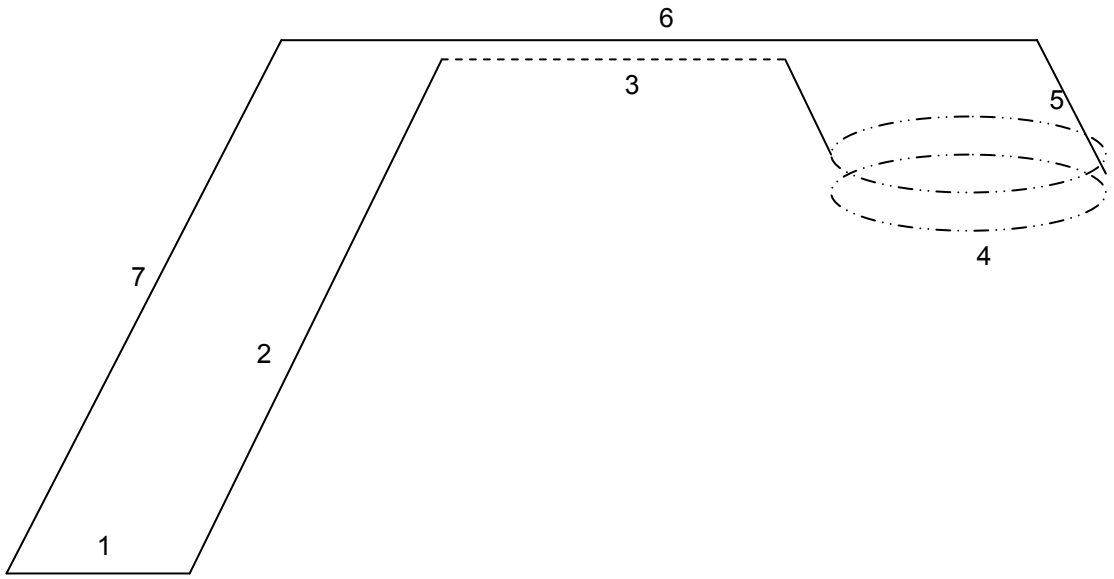

Figure 1.5: Mission Map for Point Defense Intercept: *(1) Take off and Acceleration, (2) Climb from sea-level to optimum cruise altitude, (3) Dash 200 nm at maximum speed and 35,000 ft, (4) Combat allowance, a) One sustained 360 degree turn at mach 1.2, b) One sustained 360 degree turn at mach 0.9, (5) Climb/accelerate to optimum speed and altitude, (6) Cruise back 200 nm at optimum speed and altitude, (7) Descend to sea-level, and the final requirement which is not depicted is, Reserves for 30 minutes at speed for maximum endurance.*

1.3.3. Intercept/Escort Mission

Unlike the previous two missions, this mission does not have to be completed as specified in the request for proposal. This mission was designed to determine the combat radius of the aircraft and its ability to fly at extremely low speeds which may be needed to escort civilian aircraft. The combat radius of the *Shrike* was defined using the following numbers: the dash out was a minimum of 200 nm, then the 300 nm escort was performed, and finally the aircraft cruised back a total of 500 nm. The escort Mach number was chosen to be 0.70 to 0.85 which is based off the slow cruising speeds of business jets and turboprops. Figure 1.6 shows the map for this mission.

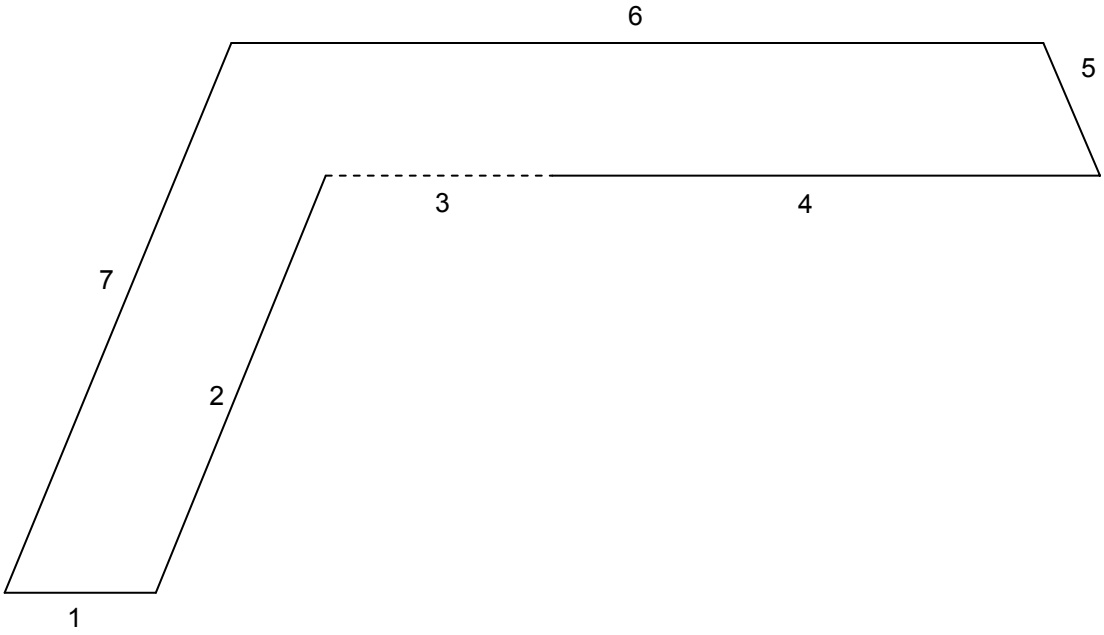

Figure 1.6: Mission Map for Intercept/Escort: *(1) Take off and Acceleration, (2) Climb from sea-level to optimum cruise altitude, (3) Dash out 200 nm at maximum speed and 35,000 ft, (4) Escort for 300 nm at minimum practical airspeed. Retain all weapons, (5) Climb/accelerate to optimum speed and altitude, (6) Cruise back 1275 nm at optimum speed and altitude, (7) Descend to sea-level, and the final requirement which is not depicted is, Reserves for 30 minutes at speed for maximum endurance.*

1.4. Point Performance and Additional Requirements

Table 1.2 shows the performance numbers that the *Shrike* achieves and uses to complete each of the three missions prescribed above. The table shows that the design performs to all the specified Mach numbers while using very achievable thrust to weight ratios and lift to drag ratios.

Additionally, the *Shrike* achieves, and exceeds, the instantaneous turn rate of 18 degrees per second with the use of thrust vectoring. Also, with the high thrust to weight ratio, the *Shrike* can easily takeoff from the prescribed 8,000 ft NATO runways with a takeoff roll of around 3,400 ft.

Table 1.2: *Shrike's* performance capabilities

Max Mach	2.2
Cruise Mach	0.8
Loiter Mach	0.8
Maneuver Mach, 1	0.9
Maneuver Mach, 2	1.2
Mach Take-off	0.34
Mach Stall	0.28
TSFC, Max	1.85
TSFC, Cruise	0.96
TSFC, 1	1.88
TSFC, 2	1.93
SFC, loiter	0.96
AR_{sub}	7.1
AR_{int}	4
AR_{sup}	2.5
T_{max}	51500 lbs
$W_{combat\ fuel}$	1572 lbs
n_{max}	7
T_{SL}/W_{TO}	0.95
W_{TO}/S	72 psf

2. Initial Concepts

Initial analysis of the mission requirements revealed that the HDI must dash at a maximum mach number of 2.2 and loiter for four hours. These two segments of the DCAP mission were considered as the driving constraints for the initial concepts. To maximize performance at supersonic speeds a short wingspan and large leading edge sweep must be utilized to drive low drag characteristics and the best performance. When in subsonic flight large wingspans give the highest L/D and greatest performance by reducing induced drag. To meet both the requirements a delta/cranked arrow, diamond, and variable sweep wing were evaluated.

2.1. Delta/Cranked Arrow

The first concept evaluated was a delta/cranked arrow configuration can be seen in Figure 2.7. The delta wing has a large leading edge sweep angle that would be beneficial at supersonic mach numbers. The large 60° sweep allows shocks originating from the nose of the aircraft to bypass the wing reducing the wave drag. The delta wing also has a compact shape and is easy to manufacture. The small support structure required provides a large amount of strength while allowing for extra room to store fuel; however subsonic flight regimes lead to many disadvantages for the cranked arrow wing. The low aspect ratio of the wing leads to high-induced drag and loss of performance during low speed maneuvers in combat. The high induced drag also increased the amount of fuel required to perform the four hour loiter mission.

A cranked arrow wing adds an extension to the wing that is at a lower leading edge sweep angle. This extension increases the span and aspect ratio leading to better performance at subsonic speeds while maintaining the benefits of a delta wing at high mach numbers. The cranked arrow also has a larger wing area that allows for more fuel and weapons to be carried extending the aircrafts range up to 125% from a conventional wing, and combat effectiveness.

INITIAL WEIGHTS AND DIMENSIONS	
W_0	45065
T/W_{max}	1.2
$T_{takeoff}$	46647
T_{combat}	23883
Area (ft^2)	1151
Span (ft)	48
Aspect Ratio	2
Leading Edge Sweep (deg)	60
t/c	0.05
Taper ratio	0.23
C_{root} (ft)	39

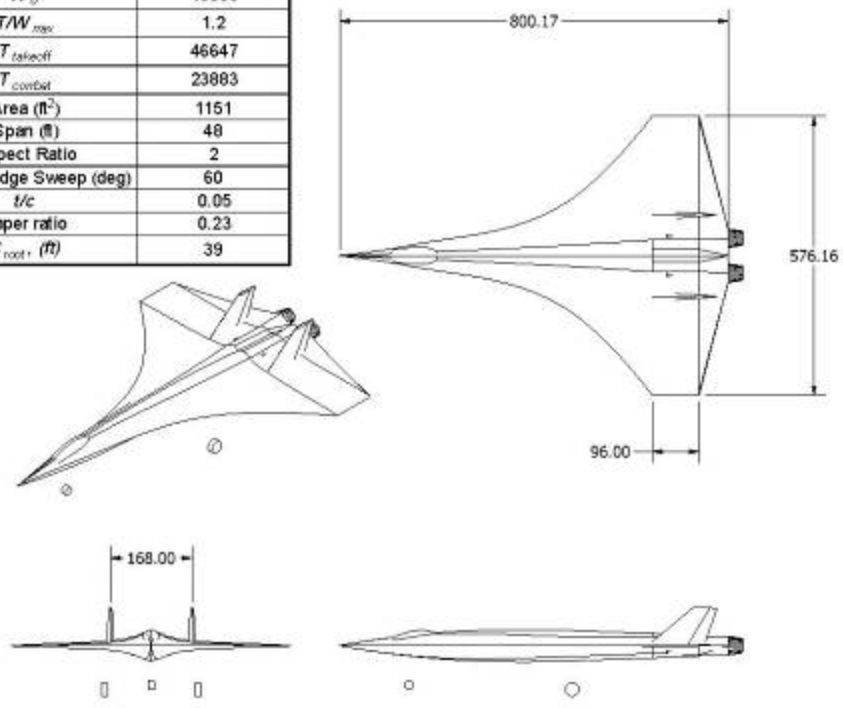

Figure 2.7: The cranked arrow configuration was discarded due to its poor performance in required maneuvers. Its fuel consumption was too large during the loiter phase of the DCAP mission. Fuel and materials needed caused an increase of weight, making this concept the poorest of the three in performance.

2.2. Diamond Wing

The diamond wing aircraft, shown in Figure 2.8 was the second design entering the HDI concept matrix. A diamond wing is a simple design that requires a minimal amount of structure. It is easy to manufacture reducing cost and weight. With an aspect ratio of 3.3 and wing sweep of 48° the diamond wing reduces induced drag during subsonic flight while still providing adequate performance at supersonic flight. Because the sweep is only 48°, shocks off of the nose of the aircraft at high mach numbers will increase the wave drag. Large engines will need to be utilized to offset the high drag resulting in more weight and a larger aircraft while weight penalties must be reduced above all parameters because of its ability to inflate the cost of an aircraft

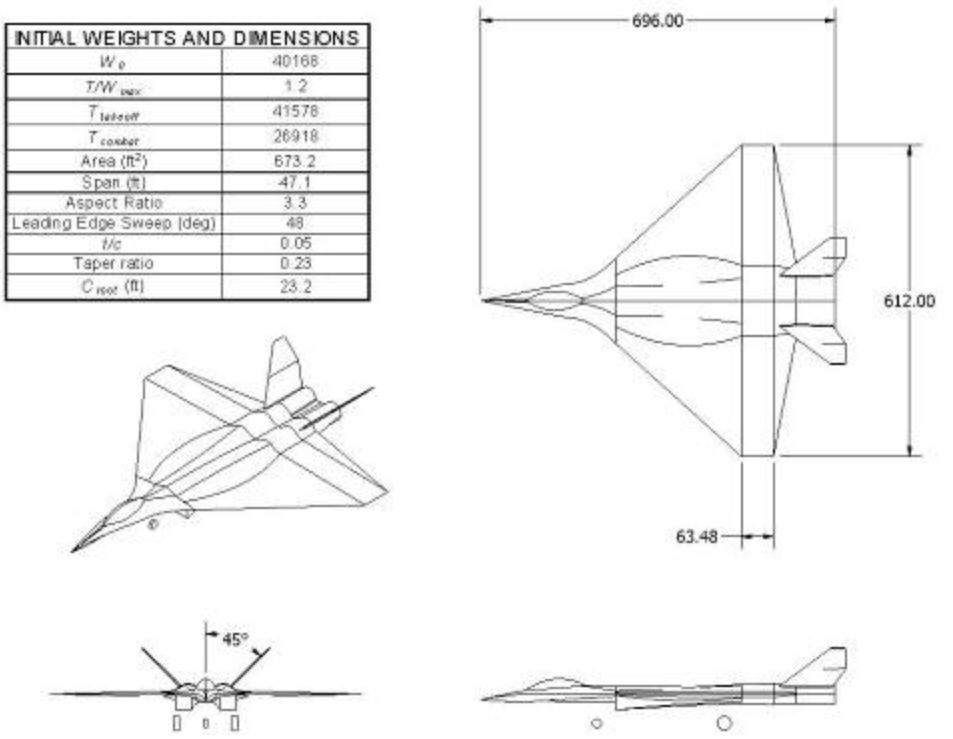

Figure 2.8: The diamond wing featured a simple design and simple structural setup. The diamond had good aerodynamics; however, did not perform as well in the I/E mission.

2.3. Variable Sweep

The variable sweep wing provides excellent performance characteristics in both supersonic and subsonic flight. During subsonic flight the wing has a leading edge sweep of 18.5° and large wingspan reducing the induced drag and yielding a high L/D. When in supersonic flight the leading edge angle becomes 65° reducing the component of air hitting the leading edge and reducing drag. The sweep back angle of 65° also allows the shocks off of the nose to bypass the wing increasing its performance; a sketch of the variable sweep design can be seen in Figure 2.9. A higher thickness to chord ratio can be utilized when sweeping the wing because in the swept back position the chord changes resulting in a smaller t/c and less drag. While in subsonic flight the high t/c allows for greater lift, strength and more room for internal fuel.

Disadvantages of the variable sweep wing are cost and complexity of the sweeping mechanical system and structure. A large and heavy wing-box must be utilized to sweep the wing resulting in an increase in weight, and thus cost. The wing-box of an F-14 is ion welded in a vacuum and made of titanium. The process provides a strong structure but at a very high cost and weight. Modern materials and structure technology have given rise to the notion

that a variable sweep wing box built with these innovations can be manufactured and constructed with less weight penalty than is seen with the F-14.

INITIAL WEIGHTS AND DIMENSIONS	
W_0	35474
T/W_{mic}	1.2
$T_{takeoff}$	36719
T_{combat}	29828
Area (ft^2)	632.9
Unswept Span (ft)	68.9
Swept Span (ft)	39.8
Unswept Aspect Ratio	7.5
Swept Aspect Ratio	2.5
Leading Edge Sweep (deg)	28
t/c	0.05
Taper ratio	0.23
C_{root} (ft)	14.9

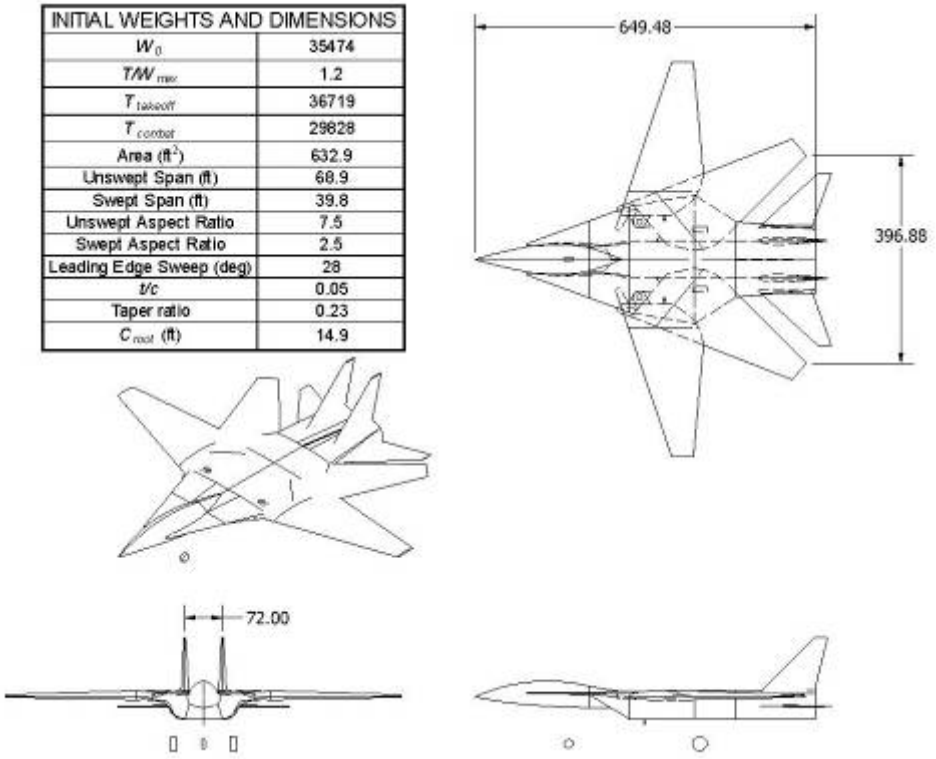

Figure 2.9: Concept of variable-sweep configuration has a more complex structure, leading to heavier fuselage section. Wings can be reduced in size compared to other concepts, reducing weigh. This design was able to out-performed other concepts in all three missions described in RFP. The variable sweep concept has the least amount of fuel needed to complete the missions.

2.4. Evaluation of Concepts

The DCAP mission was used as the sizing mission for all conceptual aircraft because of the dash and loiter requirements. Each concept was analyzed based on the power, weight, and fuel required to perform the mission.

Table 2.4 below shows the take-off gross weight of the three aircraft required for the DCAP mission. Because of the four hour loiter the cranked delta/cranked arrow configuration had to carry an additional 26,000 pounds of fuel than the diamond wing or variable sweep resulting in a take-off gross weight of 57,555 lbs. The increase in cost for the added weight and larger propulsion system outweighed the benefits of performance at supersonic speeds. The variable sweep and diamond wing designs were both close in weight and fuel usage for the DCAP mission (Figure 2.10) while the Intercept/Escort mission indicated that the variably swept aircraft used significantly less fuel and would be ideal for all mission requirements. The ability to sweep the wing allowed the variable sweep to outperform the diamond in both missions by reducing the fuel used by approximately 4,500 pounds (Figure 2.11). Table 2.3 shows the resulting fuel weights of each of the design concepts and the physical dimensions of the aircrafts as found using performance equations for each mission segment. Figure 2.10 and Figure 2.11 show the fuel consumption of each design in every segment of each mission. The Defensive Counter-Air Patrol uses the most fuel during the loiter segment.

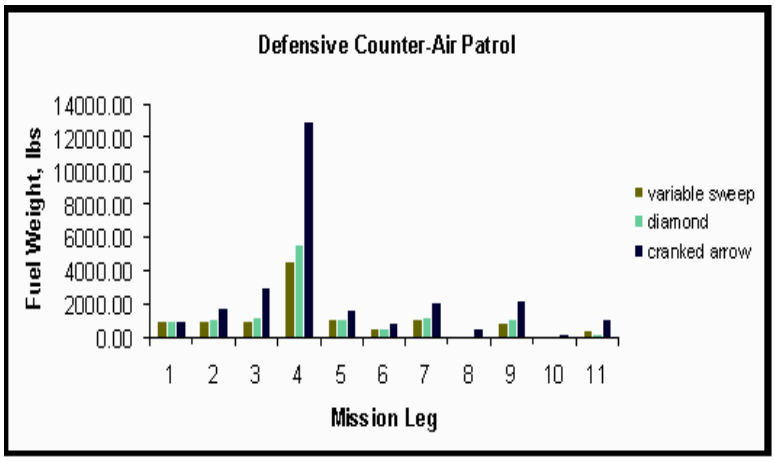

Figure 2.10: Fuel weight estimated for each segment of the DCAP mission for each conceptual aircraft where the variable sweep and diamond wing concepts outperform the cranked arrow design. Fuel weights were determined using Excel's Solver add-in and an iterative "weight build-up" method described in Raymer's Student Design handbook[1].

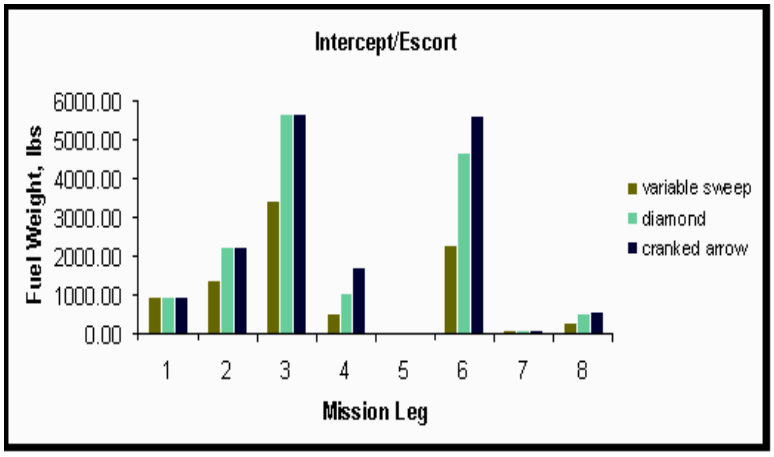

Figure 2.11: Fuel weight estimated for each segment of the I/E mission for each conceptual aircraft where the variable sweep outperforms both the diamond and cranked arrow designs. Fuel weights were determined using Excel's Solver add-in and an iterative "weight build-up" method described in Raymer Student Design handbook[1]

Table 2.3: Physical dimensions used in preliminary design calculations to find TOGW and weight of fuel consumed.

			Variable Sweep	
Concept	Cranked Arrow	Diamond	Swept	Unswept
Aspect Ratio	2	3.3	2.5	7.5
ΛLE (deg)	60	48	65	18.5
Wing Area (ft^2)	1151	673	633	633
Span (ft)	48	47	40	69
Fuselage Length (ft)	67	54	53	
TOGW (lbs)	57555	33660	31643	
Weight Fuel (lbs)	27085	12886	11477	
Thrust Needed (lbs)	69066	40392	37971.6	

Table 2.4: Evaluation matrix for the three concepts sized for the DCAP mission (Cranked Arrow, Diamond and Variable Sweep Wing) where attention is drawn to the thrust and weight required for each of the aircraft

Concept	**Cranked Arrow**	**Diamond**	**Variable Sweep**	
			Swept	Unswept
Aspect Ratio	2	3.3	2.5	7.5
Λ_{LE} (deg)	60	48	70	28
Wing Area (ft^2)	1151	673	633	633
Span (ft)	48	47	40	69
Fuselage Length (ft)	67	54	53	
TOGW (lbs)	57555	33660	31643	
Weight Fuel (lbs)	27085	12886	11477	
T/W	1.2	1.2	1.2	
Thrust (lbs) (Required)	69066	40392	37971.6	

After mission analysis structure and manufacturing of the aircraft was looked at. The cranked arrow and diamond wing configurations reduce cost since they contain simple structures relative to the variable sweep, and are

efficient to manufacture. However, advanced resin transfer molding with carbon fiber epoxy composites have reduced the cost, weight and difficulty in creating a variable sweep wing-box, while retaining the strength of titanium. It was concluded that the variable sweep concept would be a feasible as a competitive, though challenging, design to develop into a final response to the RFP.

COMPILED DATA	Appendage			
	Wing		Horizontal Tail	Vertical Tail
	Subsonic	Supersonic	-	-
Ref. Area (in^2)	84,989		18,058	17,114
Aspect Ratio	7.1	2.5	1.4	1.1
Taper Ratio	0.27		0.27	0.4
Span (in)	766.8	489.6	159.2	97.0
Root Chord (in)	170.4	354.0	73.8	126.0
Tip Chord (in)	46.3	87.6	21.2	50.4
MAC (in)	120.2	242.4	49.9	93.6
L.E. Sweep	19°	65°	48°	50°
Volume Coeff.	-		-	-
T/W Ratio	1.2			
Max TOGW (lb)	42,700			

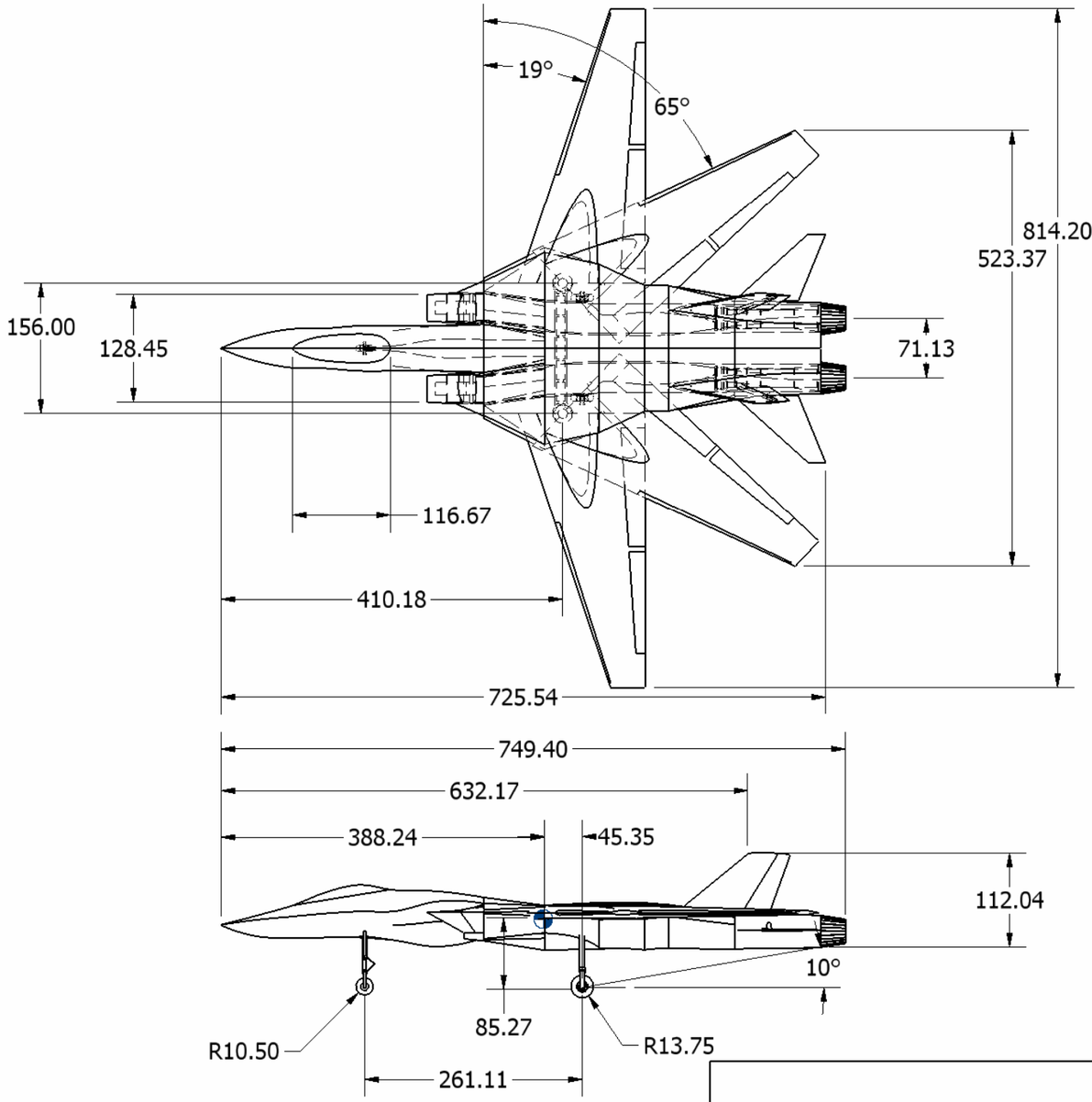

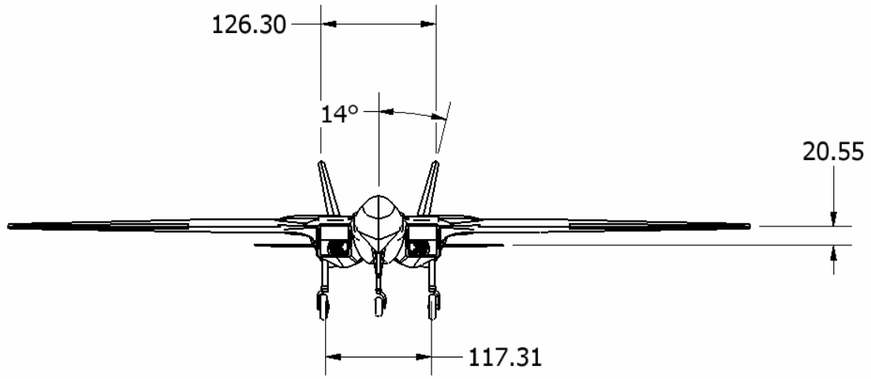

0" 100" 200" 300"

SCALE 0.01 : 1

TITLE: SHRIKE AIAA DESIGN			
SIZE: B		DWG NO: Full_Drawing	REV
SCALE		SHEET 1 OF 1	

3. Aerodynamics

Mission requirements dictate that the design has certain distinct and desirable qualities. Low drag is a necessity to reduce weight/cost while creating enough efficient lift to obtain loiter and instantaneous turn rate requirements. Further, the design must have a smooth cross sectional distribution to minimize wave drag. The intrinsic dichotomy in design requirements of efficient loiters and supersonic dash can be accomplished with improved performance and cost effectiveness through the utilization of a variably sweeping wing.

3.1. Wing Planform

The *Shrike's* planform can be subdivided into two configurations – the "subsonic configuration" and the "supersonic configuration". The reference area was predetermined through initial sizing requirements for wing loading. The subsonic configuration has features that improve loitering capabilities as well as allowance for shorter take-off/landing distances. The moderate sweep delays drag rise and the large aspect ratio combine for maximum efficiency to save valuable fuel and weight (and hence cost). Also, a taper ratio of 0.27 aides in making the lift distribution more elliptical which eliminates the need to twist the wing lowering cost and complexity when the wing is swept back. Table 3.5 shows various dimensions and parameters of both configurations.

Table 3.5: Wing specifications

	Subsonic	Supersonic
b	64.0 ft	40.8 ft
S	577.4 ft^2	668.0 ft^2
AR	7.1	2.5
λ	0.27	0.27
Λ_{LE}	18°	65°
Λ_{TE}	0°	39°
MAC	10.02 ft	20.20 ft
1/4 MAC	6.68 ft	20.48 ft
S_{wet}	1245 ft^2	

3.2. Airfoil Selection

A major advantage with having a variably sweeping wing is that the thickness remains constant while the chord increases; therefore, a higher thickness-to-chord ratio could be utilized in the subsonic configuration allowing for lower structural weight and valuable room for fuel reserves. An NACA 64-212 airfoil serves as the main wing under the subsonic planform. The 12% *t/c* wing, when swept back, yields a new *t/c* of approximately 5% which is more beneficial for supersonic flight. The smaller leading edge radius allows for vortex formation which improves the

wing's lifting capability in the supersonic regime. Figure 3.12 is a plot of the coordinates for the NACA 64-212. The airfoils used for the horizontal and vertical tails are both NACA 0006.

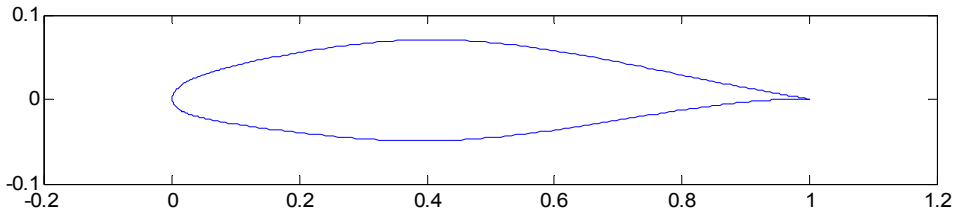

Figure 3.12: NACA 64-212 airfoil, chosen because of its historically superior performance at subsonic speeds. The tremendous thickness of this airfoil is no hindrance at supersonic speeds because the effective thickness of the airfoil once the wing is swept back becomes about five percent.

3.3.Drag Breakdown

Drag polars were assumed to be parabolic to simplify preliminary analysis. Aspect ratio and the sweep produced an Oswald's efficiency of 0.8. $C_{L\alpha}$ was estimated to be 0.0853 per degree through experimental data from Abbott and Von Doenhoff.[2] C_L and C_D for minimum drag were estimated using techniques outlined by Raymer[1] and Brandt[3] and were calculated to be 0.0426 and 0.0149 respectively. A minimized induced drag coefficient was imperative for efficient subsonic performance and was reduced to 0.0151 through airfoil selection (minimizing C_{Dmin}) and increasing Oswald's e. The following drag polar is representative of subsonic flight: $C_D = 0.0151+0.0638C_L^2-0.00544C_L$. The constants represent the induced drag, k_1 (which is merely the reciprocal of AR, Oswald's e, and π), and k_2 which is equal to $-2k_1C_{LminD}$. Figure 3.13 shows the drag polar with the corresponding $(L/D)_{max}$. Ideally, for maximum efficiency for subsonic flight the Shrike must fly at or around $(L/D)_{max}$. This translates into a cruise C_L of 0.5 which occurs at an angle of attack of 2.8°.

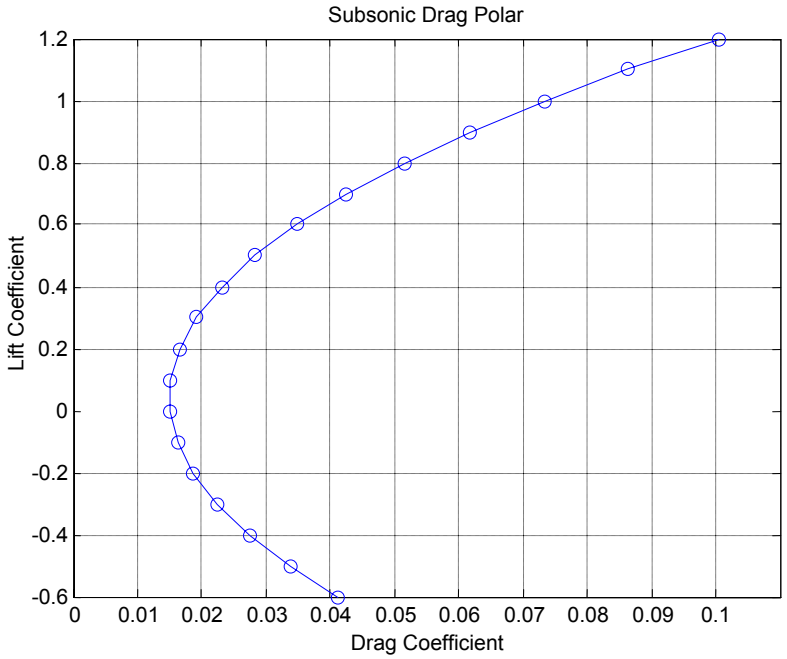

Figure 3.13: Subsonic Drag Polar at M=0.8 at an altitude of 35,000 ft.

The supersonic drag polar was similarly estimated at an altitude of 35,000 ft at a speed of Mach 2.2 and Mach 1.2. The supersonic drag polars were reduced to the following: $C_D = 0.02810+0.2306C_L^2$ for Mach 2.2 and $C_D = 0.03954+0.1003C_L^2$ for Mach 1.2. The first constant is C_{D0} including the wave drag. The k_1 values are values for supersonic speeds which are found through the relationships between AR, Mach number, and Λ_{LE}; k_2 values are assumed to be equal to zero due to the fact that generally in the supersonic regime minimum drag is achieved at zero lift at 0° angle of attack. Figure 3.14 shows the supersonic drag polar which have $(L/D)_{max}$ of 5.93 and 7.93 respectively. Unfortunately, $C_{L\alpha}$ for supersonic flight changes to 0.0356 per degree at Mach 2.2 and 0.1052 per degree at Mach 1.2 rendering an angle of attack at $(L/D)_{max}$ to be 11.2° and 5.7° which might pose possible problems near upper Mach limits.

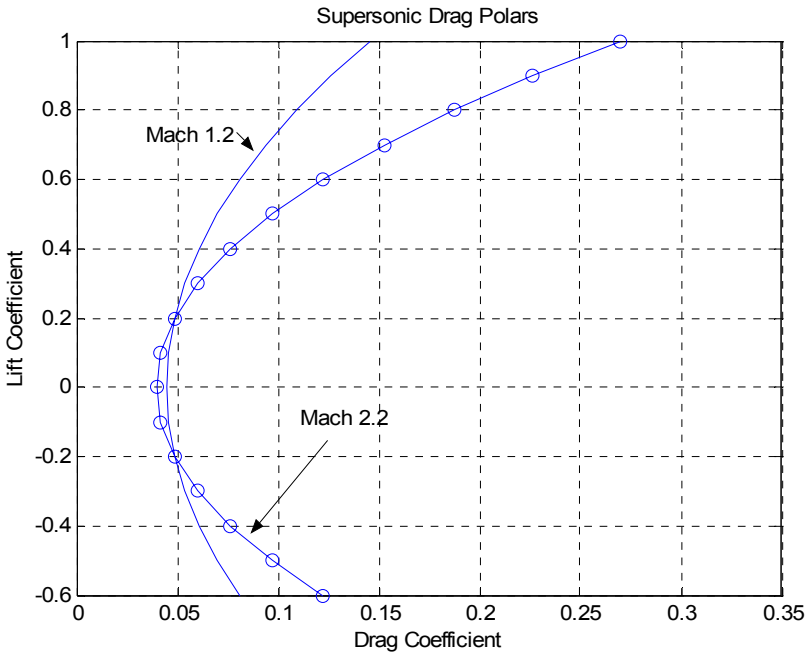

Figure 3.14: Supersonic drag polar for Mach 1.2 and 2.2 at an altitude of 35,000 ft.

The four main sources of drag can be minimized – induced, form, friction, and wave drag. The computer code FRICTION[4] was used to estimate the form and friction drags. Wave drag was estimated by the computer program AWAVE.[5] Table 3.6 shows the aforementioned drag coefficients with respect to varying Mach number.

Table 3.6: Drag breakdown of the *Shrike*

Drag	alt = 35,000 ft					
	Wave	Form	Friction	Induced	Mach #	
C_D	0	0.00006	0.00453	0.01505	0.8	
	0.014704	0.00006	0.00433	0.01505	1	
	0.0093287	0.00004	0.00305	0.01536	2.2	
						Total Drag (lb)
D	0.0	7.3	552.2	1834.7		2394.3
	2800.9	11.4	824.8	2866.8		6503.8
	8600.5	36.9	2811.9	14161.0		25610.2

Careful consideration was taken to smooth the cross-sectional area distribution of the *Shrike* in order to minimize the wave drag. Cross-sectional areas were taken from detailed drawings. Then the areas were preliminarily checked using Microsoft Excel to model a Sears-Haack body. The areas of the fuselage/components and the wing data were inputted into AWAVE and continually updated. Earlier designs produced huge drag penalties which

restricted the designs to subsonic flight; however, later designs significantly reduced the maximum cross-sectional area and greatly reduced the wave drag. Figure 3.15 shows a graph of the entire configurations cross sectional area.

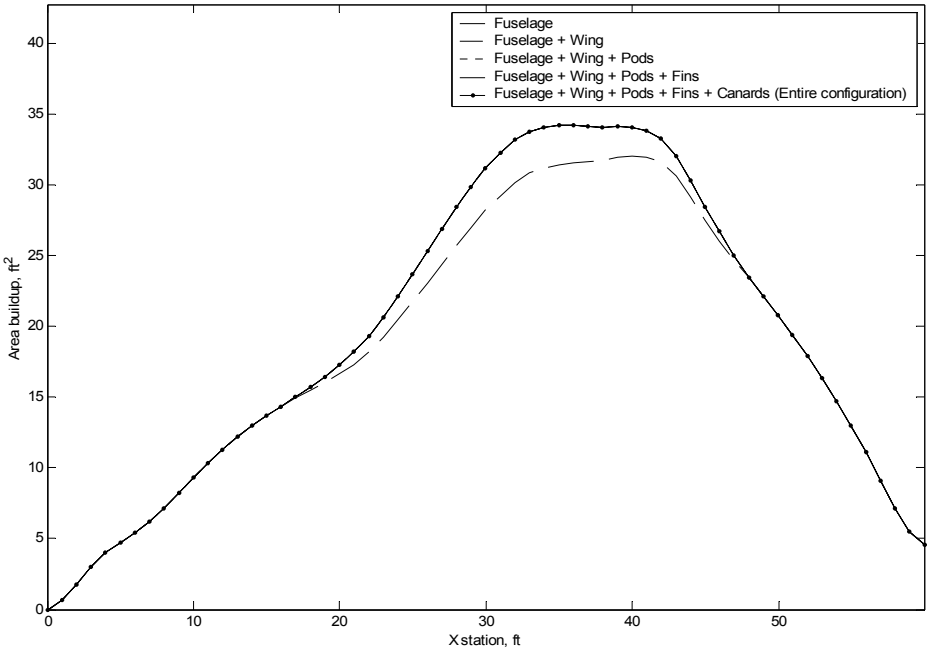

Figure 3.15: Analysis of the *Shrike's* cross-sectional area

It is evident that the *Shrike's* design was carefully tailored to closely resemble Sears-Haack distribution. The peak is slightly shifted aft due to the swept back nature of the wings and peaks at a value of approximately 33 ft^2.

It should be noted that the AIM -120 AMRAAM missiles will be semi-submerged to further decrease wave and protuberance drag while the AIM - 9M Sidewinder will be off of the body in order for the missile to be capable of sighting the target before launch.

3.4. Prediction of Lift

Airfoil section data was acquired through Abbott and Von Doenhoff's experimental data. The data suggests that at Reynolds number of around 6,000,000, there is a corresponding $C_{l,max}$ of 1.5, a lift curve slope of 0.1154 per degree and a zero-lift angle of attack of -0.5°. These values were imperative in finding three dimensional parameters such as wing-alone $C_{L\dot{\alpha}}$. To get a preliminary look at the pressure distribution along the airfoil, the inviscid code JAVAFOIL[6] was used. Figure 3.16 shows the pressure distribution over three separate angles of attack.

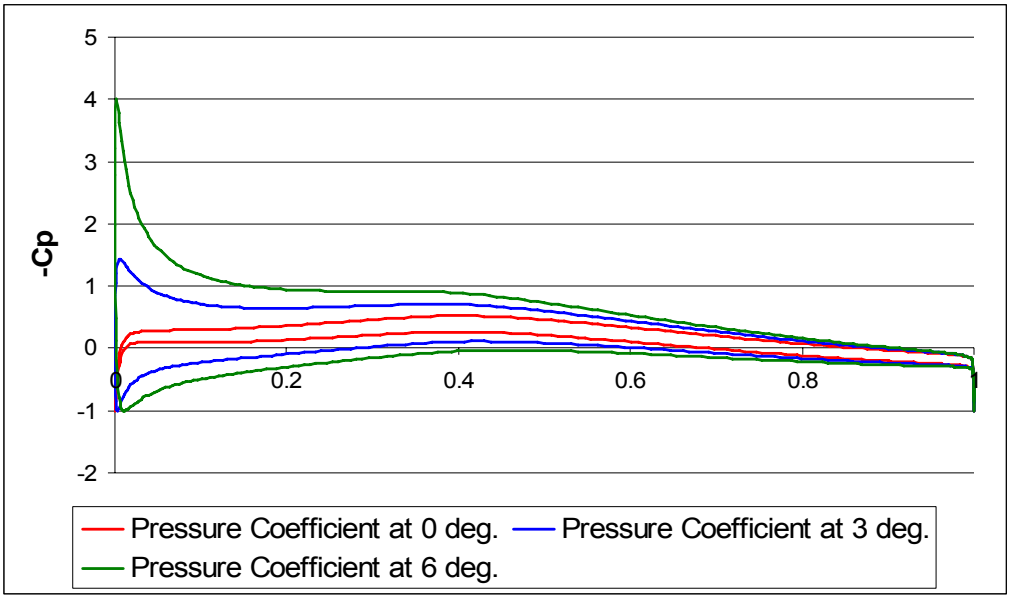

Figure 3.16: Pressure distribution over NACA 64-212 airfoil

Design requirements, especially regarding the instantaneous turn rate, dictate that C_L would need to be as high as 2.2. The ratio of the section lift coefficient over 3-D lift coefficient can be theoretically found through the taper ratio and was found to be 1.18. For low, subsonic speeds, C_{Lmax} could be as high as 1.23 without the use of leading or trailing edge flaps. This value decreases as velocity increases. Estimates from Raymer suggest that at a Mach number of 0.9, C_{Lmax} becomes 1.08. It should also be noted that the nose on the *Shrike* has a gentle sharp edge which studies have shown help vortex generation and improve lift in high speed flight. Table 3.7 shows the drop in C_{Lmax} with respect to Mach number.

Table 3.7: Estimates in change of C_{Lmax} with respect to transonic/supersonic velocities

Mach	$C_{Lmax}/C_{Lmax}(M = 0.5)$	C_{Lmax}
0.80	0.87	1.08
0.90	0.82	1.03
1.00	0.76	0.97
1.30	0.59	0.80
2.00	0.31	0.65

Utilizing thrust vectoring, the computer code TrimTV suggested that there could be an increase in effective C_{Lmax} of approximately 0.74. The lift from the tail creates an additional C_L increase of 0.2. High lift devices will also be utilized in the *Shrike's* design. Only plain trailing edge flaps and leading edge flaps were used on the Shrike.

Complicated flap devices, such as those utilized on the F-14, tend to become mechanically complex and expensive to maintain so to reduce cost, only relatively simple devices will be implemented. Furthermore, the leading edge flaps will more than likely be used during transonic flight to noticeably increase performance. The trailing edge flap will be 20% of the chord and measures approximately 16.9 ft. while the leading edge flap will measure 16 ft. across the leading edge. The high lift devices are specifically designed to produce a C_{Lmax} of 2.3 at Mach 0.8 when all flaps, including the ailerons (which act as an additional plain flap) are deflected.

3.5. Thrust-Drag Relationship

Thrust and drag data were cross-referenced in order to confirm that the *Shrike* had enough thrust to overcome the drag. The total drag was subtracted from the available thrust produced by both engines. At an altitude of 35,000 ft. and a velocity of Mach 0.8, the Shrike has 454 lbs. of excess thrust at a power setting of 4. Furthermore, a power setting of 9 at velocities of Mach 1.1 and 2.2 shows that there is 1200 lbs. and 940 lbs. of excess thrust; however, to save on fuel consumption the engines will most likely run at a power setting of 10 creating even more excess thrust. This suggests that since the drag was minimized, the benefits of vastly improved performance can be utilized using the excess thrust. Table 3.8 shows the thrust-drag relationship over several power settings.

3.6. Take-off / Landing:

The RFP had minimal take-off or landing requirements and only stipulated that the design must be capable of taking-off or landing on any NATO runway under possibly less than ideal conditions. As stated earlier, the C_L was driven up due to the instantaneous turn rate requirement and as a result, has improved take-off and landing characteristics. The drag produced at sea level at slow, subsonic speeds is approximately 7,800 lbs. while the thrust produced by the engines at a power setting of 4 is approximately 8,850 lbs. With flaps deflected and no thrust vectoring, C_{LTO} should be 1.22. Using the take-off parameter, *TOP*, the take-off distance is approximately 3,400 ft. at sea level. Stricter constrains required the additional analysis of take-off and landing at high altitudes during icy conditions. Again, due to our increased lift coefficient, detailed analysis using Raymer suggested that the *Shrike* can take-off during the aforementioned conditions over a distance of 5,700 ft and land at around 5,400 ft.

The weight of the *Shrike* will be significantly less during landing and will be able to land within a distance of 3100 ft. including a 1000 ft. additional space for a possible touch-and-go landing.

Table 3.8: Thrust / Drag Data

Mach 0.8				
PS	1 Engine (Thrust - lb.)	2 Engines (Thrust - lb.)	Tot. Drag (lb.)	T-D (lb.)
10	3,849	7,699	2,394	5,304
9	3,274	6,548	2,394	4,154
8	2,743	5,485	2,394	3,091
7	2,355	4,710	2,394	2,316
6	2,011	4,022	2,394	1,628
5	1,705	3,410	2,394	1,016
4	1,424	2,849	2,394	455
3	1,154	2,308	2,394	-87
Mach 1.1				
PS	1 Engine (Thrust - lb.)	2 Engines (Thrust - lb.)	Tot. Drag (lb.)	T-D (lb.)
10	4,511	9,022	6,504	2,519
9	3,830	7,659	6,504	1,156
8	3,203	6,407	6,504	-97
Mach 2.2				
PS	1 Engine (Thrust - lb.)	2 Engines (Thrust - lb.)	Tot. Drag (lb.)	T-D (lb.)
10	15,874	31,747	25,610	6,137
9	13,275	26,549	25,610	939
8	10,715	21,430	25,610	-4,180

4. Stability and Control

4.1. Tail Selection

In the early stages of the design, a V-tail configuration was chosen for its reduced interference drag as well as for its modern look. The lower drag, vs. a conventional tail, offered by the V-tail seemed advantageous for the design due to the extensive loitering time and supersonic speeds called for in the RFP. However, V-tails require a complex control system due to the coupled pitch and yawing moments caused by the "ruddervators" and lack longitudinal control power – vs. a conventional tail.

After further analysis, a conventional tail arrangement with twin vertical tails was chosen for the design. The conventional tail arrangement provides better pitch control with the use of an all moving horizontal stabilizer. The twin vertical tails are more effective since they are positioned away from the fuselage centerline. The final configuration of the twin tails are shown in

Figure 4.17. NACA 0006 airfoil sections were selected for both the horizontal and vertical tails based on thickness and lift characteristics.

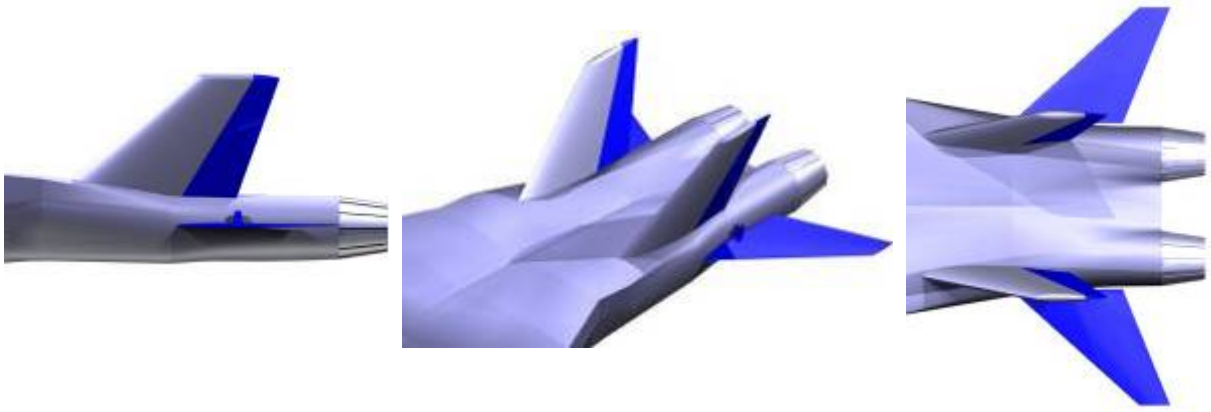

Figure 4.17: Twin Tail Arrangement

4.2. Horizontal Tail Sizing

The philosophy behind the horizontal tail sizing and placement location was to maintain a level of relaxed longitudinal stability throughout the mission phases. A low or negative static margin, SM, is necessary for this design because it improves the agility of the aircraft.

Initial horizontal stabilizer sizing was done through the methods prescribed in Raymer[1] and Roskam[7]. Raymer follows a historical trend line and provides an estimate of the center of gravity, CG, location based on inherent or relaxed longitudinal stability. The result was a tail area of 186 ft^2 with a root and tip chord of 11.9 ft and 2.19 ft respectively. This method proved inadequate because it lacked a way of determining static margin change with tail area.

Roskam[8] provides methods of analyzing tail area versus CG travel and static margin by means of longitudinal Xplots. Due to the variable wing sweep design of the aircraft a study of this effect on neutral point travel had to be made for the swept and unswept conditions. Evaluation of the static margin at aft most CG location was performed using Figure 4.18 and Figure 4.19. Clearly, Figure 4.19 shows that by sweeping the wings aft the neutral point of the aircraft is significantly moved aft resulting in a positive static margin of 3.6% at aft most CG location.

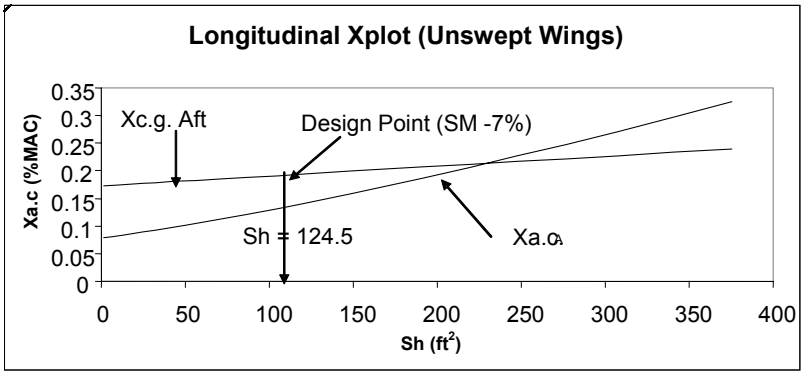

Figure 4.18: Study of tail area vs. SM in the subsonic regime (Mach 0.2)

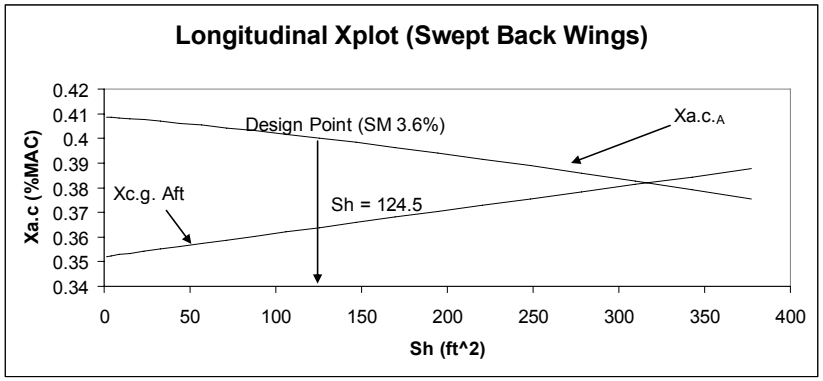

Figure 4.19: Study of tail area vs. SM in the super sonic regime (Mach 2.2)

The final horizontal tail dimensions are presented in Table 4.9 and were selected because they offered an optimum between subsonic and supersonic static margins. *Shrike's* CG locations and static margins were analyzed

for the DCAP mission and are presented in Table 4.10. The static margin values are well within the limits called for in the RFP – maximum SM ±10%.

Table 4.9: Horizontal tail dimensions

H.T. Dimensions	
CR	9.8 ft
CT	1.8 ft
b	21.6 ft
S	125.4 ft^2
λ	0.2
ΛLE	48°
AR	3.7

Table 4.10: CG and SM changes during DCAP mission

	CG Location (ft)	% Fuselage	Altitude (ft)	SM (%)
(1) Takeoff	33.36	0.561	SL	-1.8
(2) Climb/accelerate	33.5	0.563	35000	-4.8
(3) Cruise (300 nm)	33.7	0.567	35000	-6.8
(4) Patrol	33.7	0.567	35000	-6.8
(5) Accelerate	33.51	0.564	35000	0.8
(6) Dash	33.36	0.561	35000	1.6
(7) Combat	32.93	0.554	35000	3.9
(8) Climb/accelerate	32.94	0.554	35000	0.8
(9) Cruise (400 nm)	32.49	0.546	35000	5.2
(10) Descend	32.51	0.547	35000	5.2
(11) Landing	32.34	0.544	SL	8.3

4.3. Vertical Tail Sizing

The twin vertical tails were sized to provide inherent lateral stability using Roskam[8] methods. The overall lateral level of stability was assumed to be $Cn_\beta = 0.001$ per degree for sizing purposes, as explained in Roskam[8]. Analysis of tail area versus lateral stability was done using Figure 4.20 and final dimensions are shown in Table 4.11.

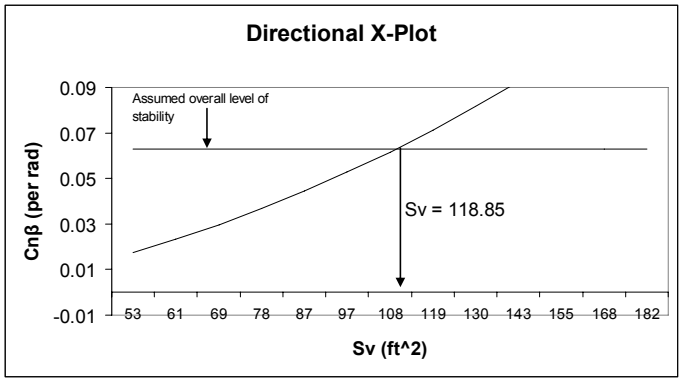

Figure 4.20: Lateral stability vs. vertical tail area

Table 4.11: Dimensions are for one of two vertical tails

V.T. Dimensions	
CR	10.5 ft
CT	4.2 ft
b	8.09 ft
S	59.42 ft^2
λ	1.1
ΛLE	50°
AR	0.4

4.4. Control Power Assessment

The horizontal tail must have sufficient power to trim the aircraft at all conditions as well as rotate the nose during takeoff. The nose-wheel rotation during takeoff requires the most control power, thus, it was checked using the spreadsheet CPRCheck[8] and the results are shown in Table 4.12. It is apparent that the all moving horizontal tail provides sufficient control power to rotate the aircraft during takeoff; the nose-wheel may start rotating at 187.19 ft/sec.

Table 4.12: Nose-wheel rotation during takeoff

Nose Wheel Lift-off	
V (ft/s)	AOA (deg)
184.14	0
187.19	1.12
190.24	3.57
193.29	6.91
196.35	10.95
199.41	15.31
202.48	19.55

Shrike is a twin-engine aircraft and as such the twin vertical tails must provide sufficient control power to trim the aircraft if one of the engines were to fail. A rudder of 30% chord length and same span as the vertical tail is used to trim the aircraft during engine-out conditions. Roskam[10] methods were used to analyze the control power requirements along with JKayVLM[9] to estimate $Cn_{\delta r}$. The vertical tails provide enough power to trim the aircraft with a rudder deflection of 12° at landing conditions.

Roll performance is specified in MIL-F-8785C and to meet them *Shrike* utilizes inboard flaperons as well as outboard ailerons. Both of the control surfaces are sized at 20% wing chord in width and start at 25% *b*/2 to 60% *b*/2 and 61% to 95% *b*/2 for the flaperons and ailerons respectively. Equations outlined in Roskam[10] were used to calculate the roll performance at 20° deflection of both flaperons and ailerons. Table 4.13 has the required and actual times to bank angle for the aircraft. *Shrike* meets all level 1 handling requirements for roll performance

Table 4.13: Roll performance

Roll Performance Class IV			
Handling Level		Time to Bank 90° (s)	
		Required:	Actual:
Level 1 (A)	Air Combat	<1.1	0.6
Level 1 (B)	Cruise	<1.7	0.78
Level 1 (C)	Takeoff/Landing	<1.1	0.94

4.5. Dynamic Stability

Shrike was designed to be longitudinally unstable, thus, a Stability Augmentation System (SAS) is used to stabilize the aircraft. If SAS was not to be implemented then *Shrike* would not able to meet military specifications for Phugoid and Short Period mode. Dynamic longitudinal stability was checked for the cruise and takeoff/landing flight conditions. Roskam[9] and JkayVLM[9] were used to approximate the required dynamic stability and control derivatives. Table 4.14 shows that the aircraft meets Level 1 requirement's except for the Phugoid mode in takeoff/landing; Level 2 handling quality was achieved during takeoff/landing. Angle of attack and pitch rate feedback were utilized to obtain the stability values shown in Table 4.16. The required feedback gain values are shown in Table 4.15 and are well below the maximum gain values of K_α = 5 deg/deg and K_q = 2 deg/deg/sec as specified in Roskam[10].

Table 4.16: Longitudinal dynamic stability

Mode	Requirement	Cruise	Feedback Gain
Phugoid (Level 1)	$\zeta p > 0.04$	0.04	
Short Period (Level 1)	$0.30 < \zeta sp < 2.0$	0.8	Kq = 0.95
(rad/sec)	$1.3 < \omega sp < 8$	3	$K\alpha = 1.50$
Mode	Requirement	Takeoff/Landing	Feedback Gain
Phugoid (Level 2)	$\zeta p > 0$	0.017	
Short Period (Level 1)	$0.35 < \zeta sp < 1.30$	1	Kq = 0.81
(rad/sec)	$1.4 < \omega sp < 8$	4	$K\alpha = 2.89$

As previously discussed the aircraft was designed as laterally/directional stable. The twin vertical tails were designed to stabilize the airplane without any stability augmentation systems. Lateral dynamic stability must be checked through Spiral, Dutch Roll and Roll mode as specified in Military requirements. Table 4.17 lists the dynamic stability requirements as well as *Shrike*'s performance. Spiral and Roll mode Level 1 specifications were achieved for both cruise and takeoff/landing. *Shrike's* Dutch Roll did not meet minimum Level 1 damping ratio but does meet Level 2 requirements which will not significantly affect its performance.

Table 4.17: Lateral dynamic stability

Mode	Requirements	Cruise	Takeoff/Landing
Spiral (Level 1)	Tr > 12 sec	34.2	44.2
Dutch Roll (Level 2)	$\zeta dr > 0.02$	0.034	0.07
(rad/sec)	$\omega ndr > 0.4$	1.081	0.9
Roll (Level 1)	Tr < 1.0 sec	0.78	0.94

Overall, *Shrike* meets – and in most cases exceeds – all required specifications as outlined in MIL-F-8785-C and it's capable of successfully completing all missions as called for in the RFP.

5. Propulsion

5.1. Engine Selection

A low bypass-ratio turbofan engine with afterburner is selected to power the *Shrike* interceptor. This type of engine provides the best balance for meeting the high mach number and extended loiter time requirements of the RFP. A thrust to weight ratio at takeoff of 0.95 was found by making a thrust-to-weight versus wing-loading diagram of the constraints required by the RFP. With a takeoff gross weight of 42,000 lbs, the total thrust needed at takeoff is 39,900 lbs. The Pratt and Whitney F-135 and General Electric F-136 engines are in the 40,000 lbs thrust range and could be used to meet the requirements for a single engine design. However, the engines are new and little performance information is available about them and so they were eliminated from selection. Since one engine required scaling up of about 24% to get 39,900 lbs of thrust a two engine design will be utilized with each engine needing 19,950 lbs of thrust. To count for installation losses a 7.3% increase in thrust was added resulting in 20,090 lbs needed for take-off. This made sure that once an engine was selected it could withstand 7.3% losses at take-off and still have the required thrust. The engine matrix below Table 5.18 provides several engines that meet the performance requirements of the *Shrike* interceptor and are scaled to provide the required take-off thrust. The engines were all scaled to the same thrust to give an even comparison in other characteristics. Since area ruling is affected by the volume of the engine and aircraft weight is affected by engine weight and SFC they were the main driving criteria for selection.

Table 5.18: Specifications of low bypass ration turbofan engines with afterburner[10]

Engine	Max Thrust (lbs)	Max Power TSFC (1/hr)	Dry Weight (lbs)	Length (in)	Max Diameter (in)	Bypass Ratio	Volume (ft3)	Percent Scaled	Current Platform
F110-GE-129	21,407	1.9	2,830	161	40	--	116	-27%	F-16 F-15
F110-GE-132*	21,407	2.09	2,583	154	38	0.68	101	-33%	F-16
F100-PW-229	21,407	--	2,642	168	40	0.36	121	-27%	F-16 F-15
RR EJ200	21,407	1.73	2,074	154	28	0.4	56	-5%	Euro-fighter
AIAA	21,407	1.71	2,332	145	34	--	77	-5%	--

The Pratt and Whitney, and General Electric engines were eliminated first due to their large size, weight, high SFC, and the need to scale them down roughly 30%. The RR EJ200 and AIAA engine had identical SFC values, however, the RR EJ200, shown below in Figure 5.21, was chosen since it saved forty cubic feet in volume and six hundred pounds in weight with the two engine configuration.

Figure 5.21: Rolls Royce EJ200 Low bypass ratio engine with afterburner[11]

The EJ 200 has a Full Authority Digital Control System to manage the engine, fuel flow and nozzle area, while an Engine Monitoring Unit is used to manage the state of the engine and make sure it is running properly. The EJ 200 also has a 30% increase in performance planed for the future upgrades that will result in a maximum thrust of 27,000 lbs and lower maintenance due to better parts.[12]

5.2. Inlet Design

The *Shrike* interceptor will need to perform at both supersonic and subsonic speeds so a 2-D external compression inlet will be utilized. The 2-D ramp is selected over a conical inlet because of its ease of manufacture and lower drag at speeds below Mach 2.2.[2] The inlet will have two variable geometry ramps, as shown in Figure 5.22 below, in order to create two oblique shocks followed by a normal shock.

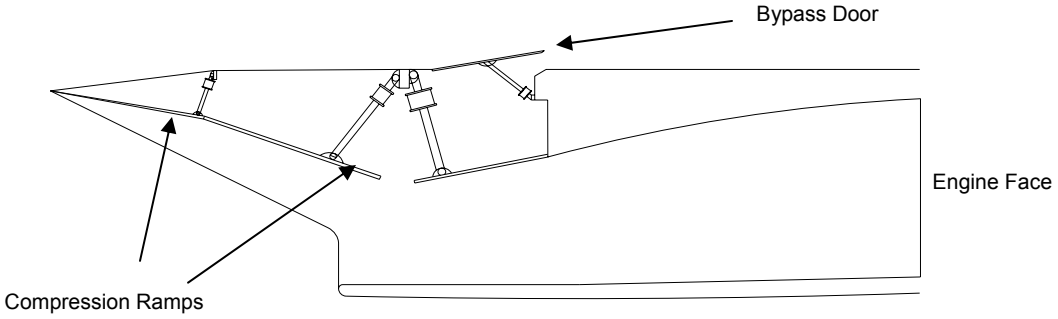

Figure 5.22: 2-D external compression inlet at Mach 2.2

The shocks will slow the air at the inlet from supersonic speed to the desired subsonic speed of Mach 0.4-0.5 at the entrance to the compressor. The ramps are scheduled to change angle based on the free stream Mach number.

Both ramps start at zero degrees at subsonic speeds and Mach 1 and deflect to ten degrees each at Mach 2.2.[2] Figure 5.23 shows the pressure recovery of the *Shrike* inlet vs. the pressure recovery as required by MIL-E-5008B based on the ramp schedule.[2] The pressure recovery of the *Shrike* inlet exceeds the recovery specified by MIL-E-5008B significantly from Mach 1 to Mach 2.2.

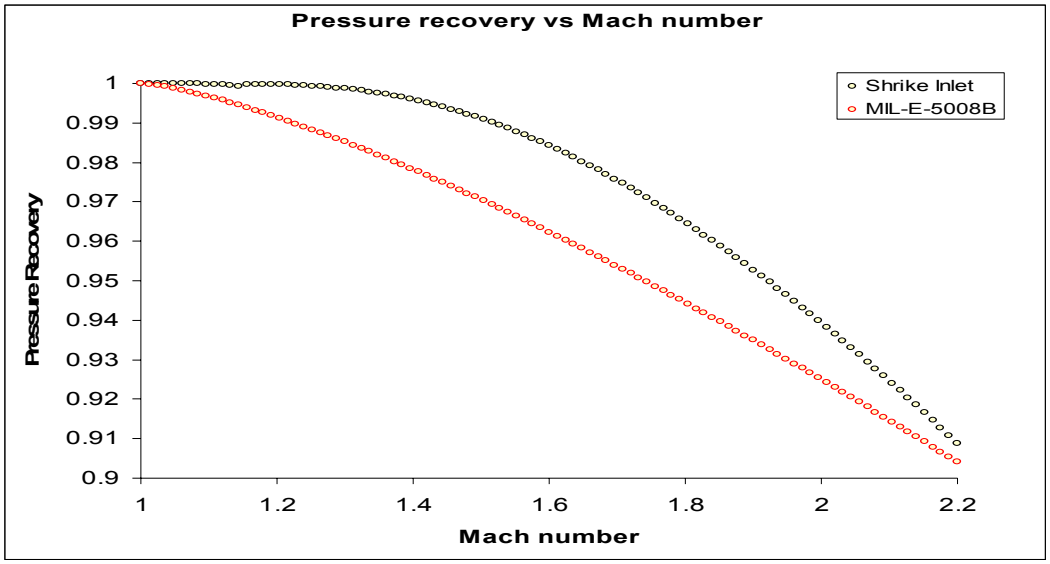

Figure 5.23: *Shrike* inlet pressure recovery vs. military requirements

The capture area is sized to be 6.89 ft^2 and includes a 4% increase of the required area to allow for the bleed of boundary layer build up inside the inlet. At speeds below the design Mach number the excess air will be bypassed through a bypass door on the top of the inlet.[2] The required airflow A_0/A_1 was found using equations 5.3 and 5.4 along with the geometry of the inlet.

$$\frac{A_{0i}}{A_s} = \frac{P_{ts}}{P_{t0}} \frac{\left(\frac{A}{A^*}\right)_{M0}}{\left(\frac{A}{A^*}\right)_{Ms}} \qquad \textbf{(5.3)}$$

$$\frac{A}{A^*} = \frac{1}{M}\left\{\frac{2}{\lambda+1}\left(1+\frac{\lambda-1}{2}M^2\right)\right\}^{\frac{\gamma+1}{2(\gamma-1)}} \qquad \textbf{(5.4)}$$

Equation 5.3 is a function of the flow properties of the free stream airflow and airflow at the normal shock. Equation 5.4 also includes the pressure recovery of the inlet P_{ts}/P_{t0}. The area ratio A_s/A_1 was then multiplied by A_{0i}/A_s to get A_0/A_1. A_s/A_1 was calculated from the inlet geometry where A_s is the area at the normal shock and A_1 is the capture area.

The inlets will be located slightly forward of and under the wing on either side of the fuselage. Because of their large size it did no seem practical to locate them under the fuselage of the aircraft. Side inlets also eliminate the need for added structure and weight since the landing gear does not need to be stored underneath them. Since the engines were spaced with a distance of three feet between them side inlets allowed for straighter ducts to the engines minimizing losses. A five inch boundary layer diverter will separate the inlet from the fuselage and stop any boundary layer build up from the nose of the plane entering the inlet. Foldout 1 shows the location of the inlet on the *Shrike*.

5.3. Exhaust Nozzle Design

Afterburning engines require exhaust nozzles that are 1.2-1.5 times the size of the capture area, while without afterburner the nozzle is 0.6-0.8 times the capture area.[2] The *Shrike* will use a converging-diverging 3-D thrust vectoring nozzle as shown in Figure 5.24 below.[2]

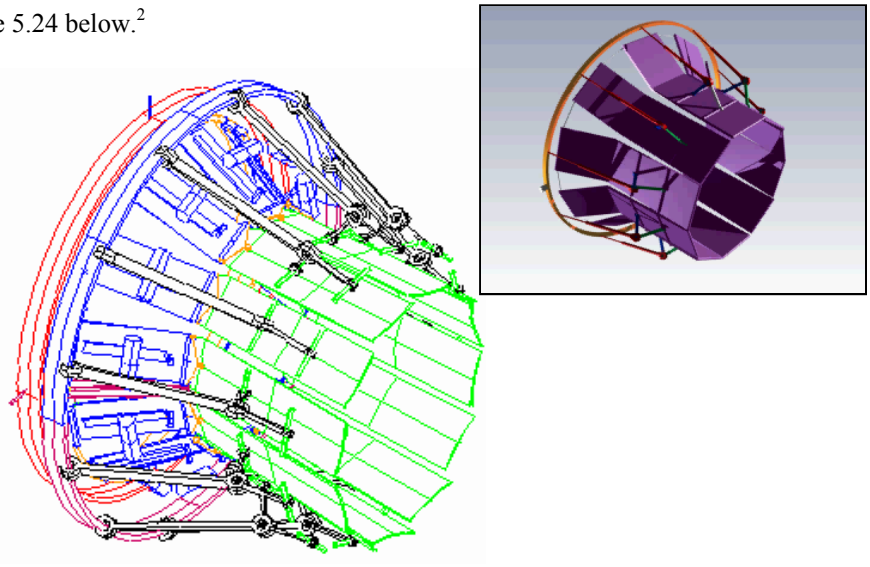

Figure 5.24: Thrust vectoring convergent-divergent nozzle for the *Shrike* interceptor.

The thrust vectoring nozzle was first tested in 1998 and is built specifically for the RR EJ200.[2] The nozzle helps meet the instantaneous turn rate required by the RFP and lower drag during flight by reducing the deflections of other control surfaces. Geometry of the nozzle was computed using the NOZZLE program developed by Jack Mattingly.[2] The area of the nozzle was found to range from a subsonic minimum of 3.26 ft^2 to a supersonic maximum of 11.1 ft^2 at Mach 2.2 and 35,000 ft.

5.4. Installation Losses

Installation losses were calculated for the interior and exterior portions of the inlet along with the exhaust nozzle. Exterior inlet drag was computed using (5.5,[2]

$$\phi_{inlet} = \frac{(P_e / P_0 - 1)(A_e / A_0)}{(Fg_c / m_0 a_0)(\gamma M_0)} \qquad \textbf{(5.5)}$$

which is a result of the oblique shock created by the leading edge lip of the inlet. Subsonic and supersonic inlet losses were computed using equations 5.6 and 5.7.

$$\phi_{inlet_{Subsonic}} = \left[\frac{M_0}{M_1}\sqrt{\frac{T_1}{T_0}}\left(1+\gamma M_1^2\right) - \left(\frac{A_1}{A_0}+\gamma M_0^2\right)\right] / \left[(Fg_c / m_0)(\gamma M_0 / a_0)\right] \qquad \textbf{(5.6)}$$

$$\phi_{inlet_{Supersonic}} = \left(\frac{A_1}{A_0}-1\right)\left\{M_0 - \left(\frac{2}{\gamma+1}+\frac{\gamma-1}{\gamma+1}M_0^2\right)^{1/2}\right\} / \left[(Fg_c / m_0)(\gamma M_0 / a_0)\right] \qquad \textbf{(5.7)}$$

which are a function of air flow, mach number and altitude and ranged from 1% to 6% which were within the predicted values of 7.3%. The largest decreases in thrust occurred at supersonic mach numbers and during takeoff. Auxiliary doors open on the side of the inlets during takeoff to allow for the required air needed, and help reduce the installation losses.

Reductions in thrust caused by the nozzle were computed using the methods in *Aircraft Engine Design*, by Jack Mattingly and were greatest at high mach numbers. Boattail drag from the large angles of the expanding nozzle attributed to the highest amounts to nozzle losses.

After the thrust reduction from the nozzle and inlet were taken into account the installed thrust of the *Shrike* engine has 20,762 lbs at sea level. The installation thrust loss was subtracted from the manufactures uninstalled thrust of 22,250 lbs. Since the required thrust is 20,090 lbs at take-off the engine provides more thrust than needed and it was chosen no to scale the engine. The engine would only be able to be scaled down a small amount creating minimal benefits in weight and volume and the need to scale the engine deck reducing its accuracy. Table 5.19 below shows specifications for one engine during selected segments of each mission.

Table 5.19: Specification of EJ200 engine at various mach numbers and altitudes.

Segment Mach# @ alt	Installed Thrust (lbs)	SFC (1/hr)	Volume (ft3)	Weight (lbs)	Cost (Million $)
Takeoff	20,762	1.73	72	2180	4.23
Cruise M0.8 @ 40k	2,823	0.9	72	2180	4.23
Loiter M0.8 @ 40k	2,823	0.9	72	2180	4.23
Dash M2.2 @ 35k	28,708	1.9	72	2180	4.23

Figure 5.25 and Figure 5.26 shown below; give the installed thrust and TSFC at maximum power, while Figure 5.27 and Figure 5.28 show installed thrust and TSFC at military power. Lines shown in red represent performance altitudes stated by the RFP.

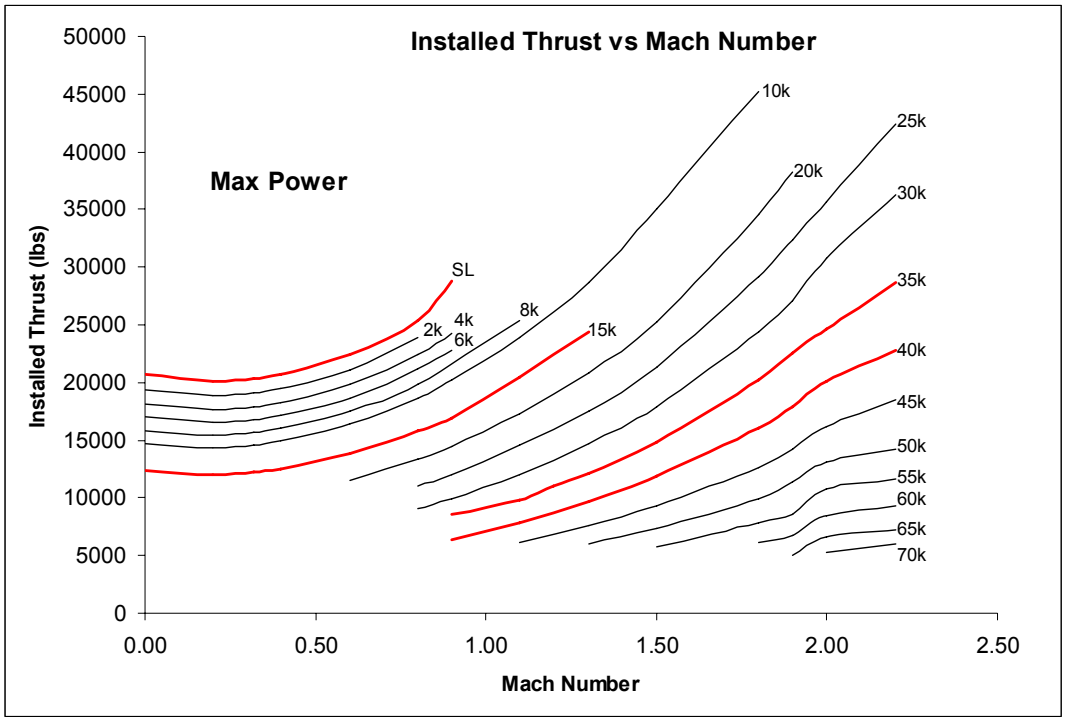

Figure 5.25: Installed Thrust vs. Mach number at Maximum Power *(Altitude is in feet)*

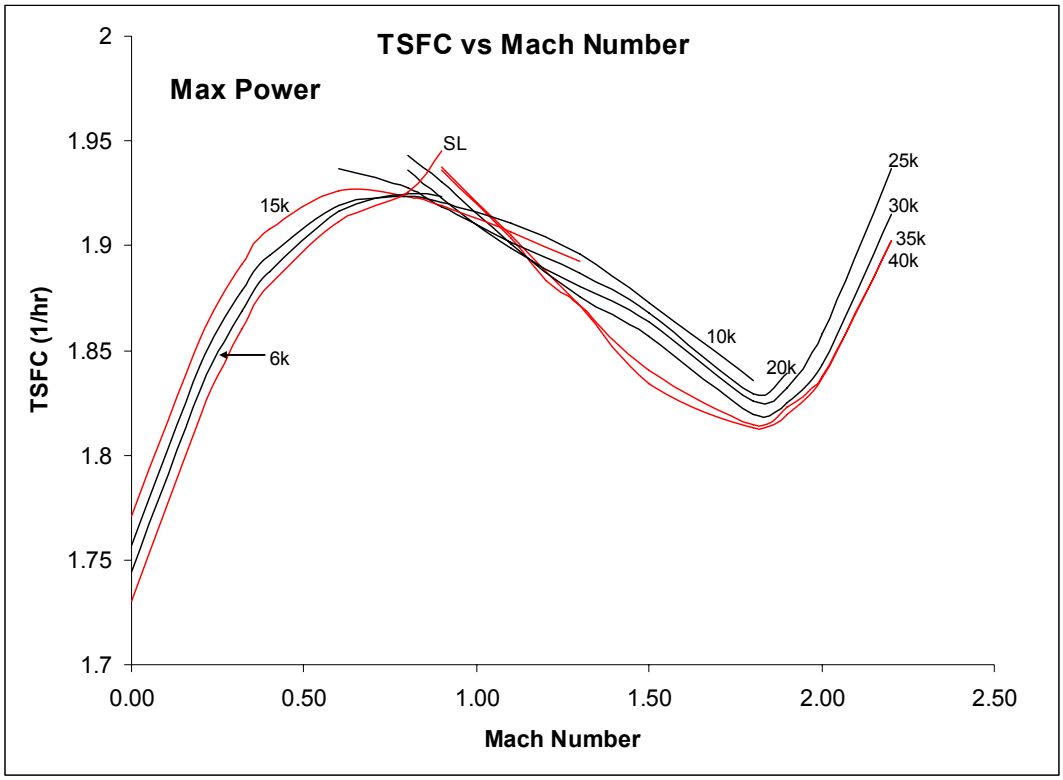

Figure 5.26: Installed TSFC vs. Mach Number at Maximum Power *(Altitude is in feet)*

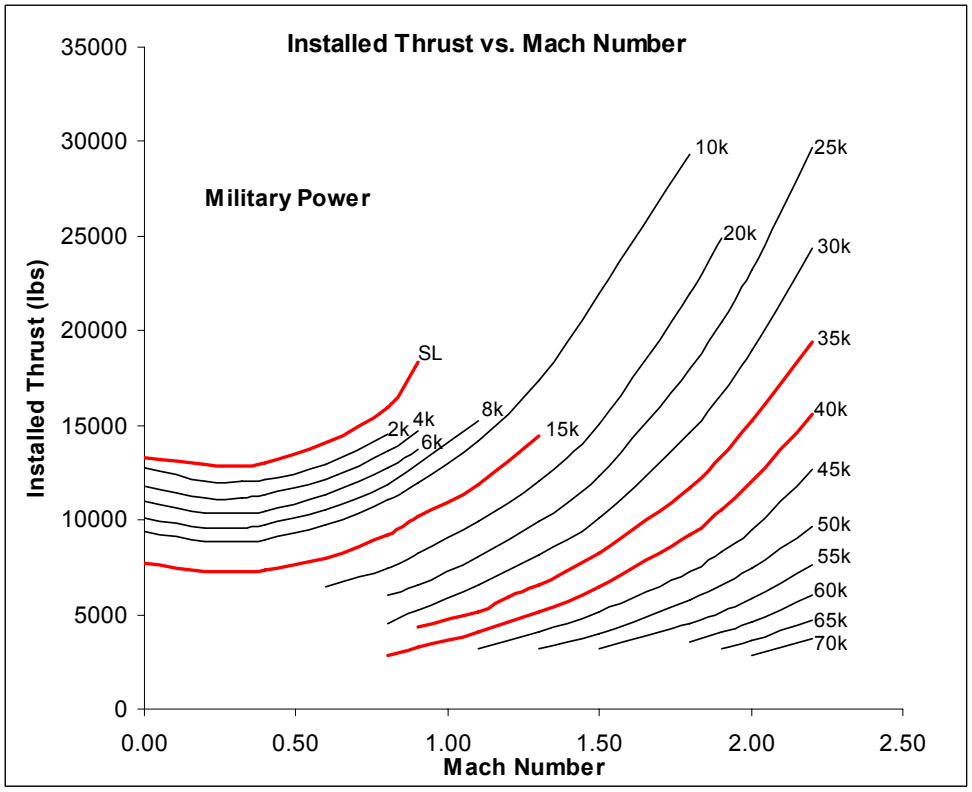

Figure 5.27: Installed Thrust vs. Mach Number at Military Power *(Altitude is in feet)*

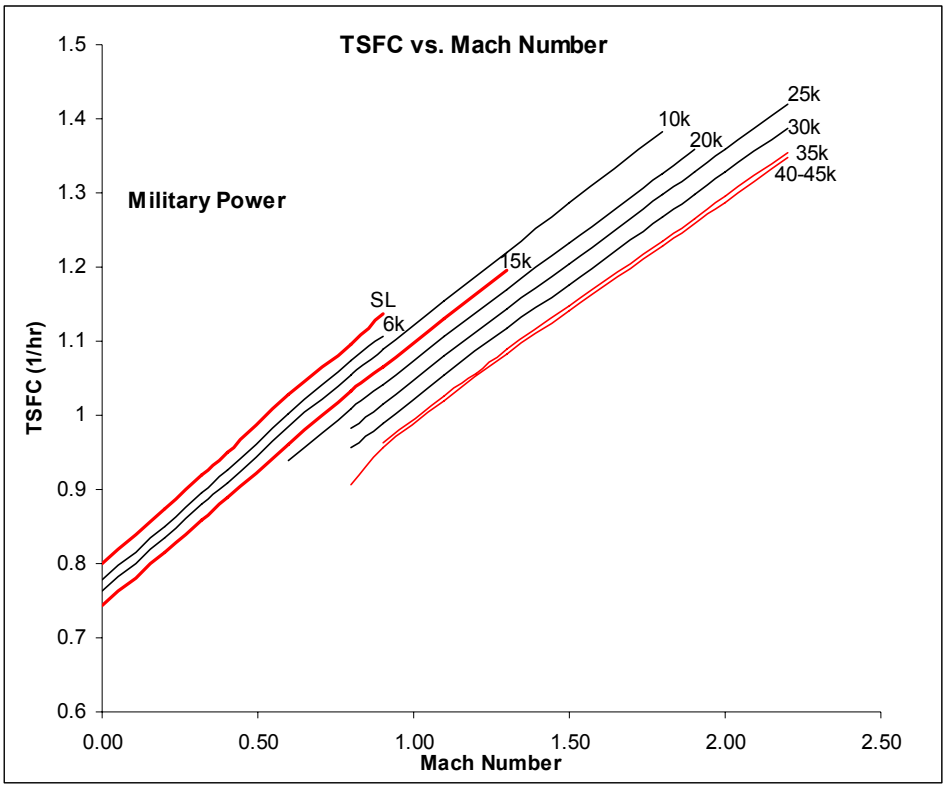

Figure 5.28: Installed TSFC vs. Mach Number at Military Power *(Altitude is in feet)*

5.5. Engine Maintenance

All systems are located on the bottom of the engine and in a one deep configuration so one part does not have to be removed to get to another. Small maintenance panels allow access through the bottom of the aircraft to all the systems. The engine will be mounted on rails in an engine bay and fixed by six points to the three supporting bulkheads. The engine will slide out the rear of the bay onto a specialized engine cart that has similar rails mounted on it as shown in Figure 5.29. The cart can be adjusted on six axes to properly align the engine with the internal rails. It is 13 ft long and can lift the engine to a height of 6 ft above the ground. Rear removal requires no large doors cut into the bottom of the aircraft that can reduce the strength of the structure.

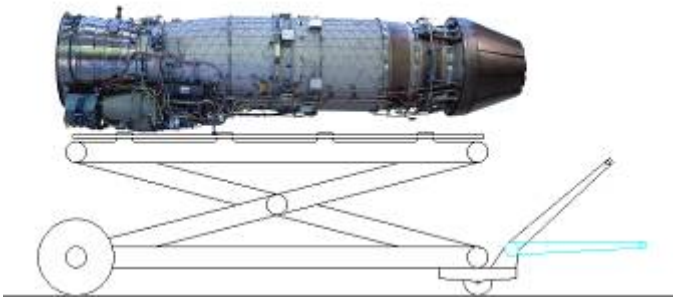

Figure 5.29: Engine Removal Cart

6. Materials and Structure

The Inland Defense Interceptor RFP required an aircraft to perform high wing loading maneuvers. To satisfy these performance criteria, a mixture of metal and composites based on strength, weight, and cost were chosen for the aircraft.

6.1. Material Selection

6.1.1. Metals

Common metals used in many aircraft are aluminum alloys and titanium alloys. These materials offer excellent properties for aircraft, but both carry some negative effects as well. As time progresses, better alloys are being produced. An aluminum lithium alloys are used by the Department of Defense due to their low density, high specific modulus, and excellent fatigue.[12] Disadvantages to this material include the need for cold work to peak properties and accelerated fatigue crack extensions when the cracks are small. The cost of Al-Li alloys is typically three to five times that of traditional aluminum alloys. This is due partly to the relatively high cost of Lithium and also to high processing and handling costs for the material.[13] However, by 2010, this material may be more widely used, lowering cost to manufacture and maintain.

Titanium alloys are also used on various components of aircraft due to their strength to weight ratio, which is the highest of all metals. However, the large density of this material limits the amount that can be applied to aircraft. An alpha-beta alloy is strengthened by heat treatment and aging, allowing them to be the prime choice in aircraft and aircraft turbine components.[14]

6.1.2. Composites

As time progresses, composites are becoming a better choice of material to use for aircraft. Composites are lightweight, thin, and also have excellent properties. The cost of manufacturing a part of composites is high today, but strategies are being taken to reduce this cost, such as the increasing use of them in aircraft. Advances in technology have also allowed composites to require much less maintenance as metals demand due to the absence of cracks. Composites are starting to be more widely used. For fighter aircraft, the F/A-22 Raptor contains the highest percentage of 24% composite material over the entire aircraft. Helpful characteristics include fiber alignment, which can increase tensile and compression strengths in desired directions as well as nullify the effects of flutter.

In recent years, an advanced resin transfer molding (RTM) process has been under development by the company Dow-United Technologies. The classic RTM process includes shaping carbon fibers in a heated mold cavities, and then injecting resin. The new process consists of taking untreated carbon fiber plies and shaping these into the complex shapes, while these are still pliable. The amount of fibers used has also been increased in the new method from 30 to 50 percent of the composite to now greater than 58 percent. These resulting carbon composites also are made to tolerances between ±0.005 to ±0.05 inch on dimensions. The advanced method results in strength properties greater than titanium and at a reduction in price if used to produce a large amount. With the request of 1000 aircraft to be made, this cost will result in being significantly smaller than the cost of using titanium in the aircraft. This new process is being applied to the F/A-22 Raptor, replacing the titanium components due to these excellent traits.[15] Properties of materials used and their placement are shown in Table 6.20 and Figure 6.30. Aircraft steel is used as a comparison.[16]

Table 6.20: Material Properties

Materials	Density (lb/in^3)	Ultimate Tensile Strength (ksi)	E (10^6 psi)	G (10^6 psi)	E/ρ	G/ρ
Aircraft Steel	0.281	-	30	11	106.76	39.14
Aluminum 2017	0.101	26	10.4	3.95	102.97	39.1
Aluminum 2024-T3	0.1	70	10.6	4.06	106	40.6
Ti-6A1-4V	0.16	138	16	6.2	100	38.75
Aramid-epoxy	0.052		11.9	4	228.84	76.92
Carbon Fiber/Epoxy Sheet	0.058	87	10.2	0.725	175.86	12.5
Carbon Fiber/Epoxy rod	0.058	217.6	18.9	-	325.86	-
Advanced RTM	0.053	-	~20	-	~377.35	-

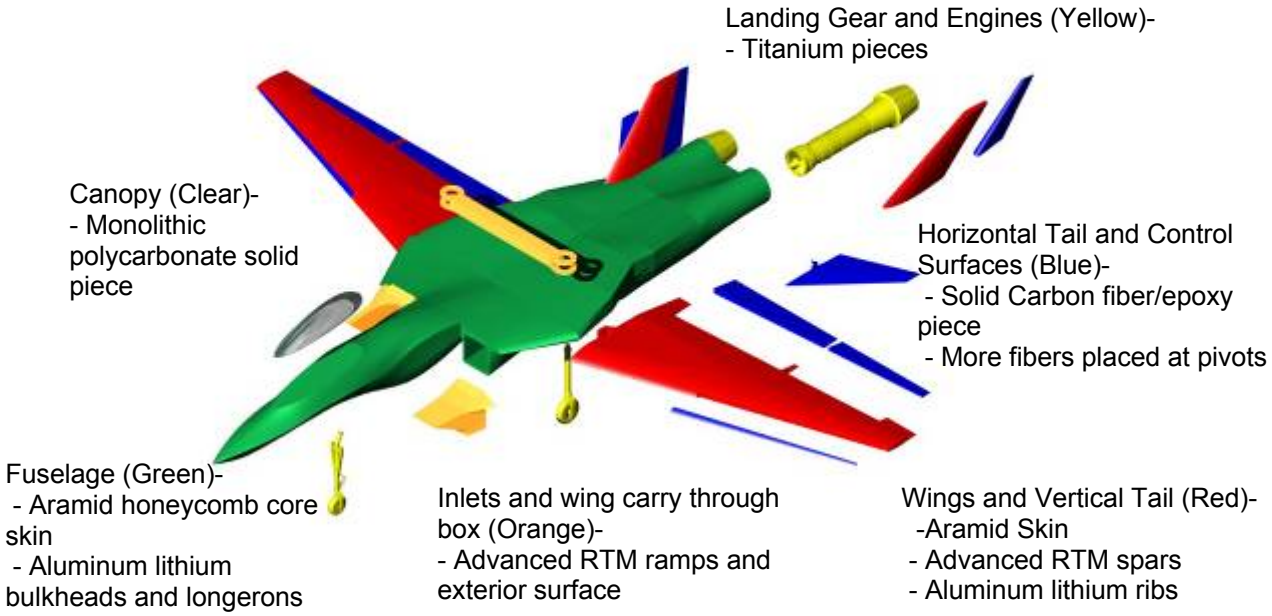

Figure 6.30: Material placement

6.2. V-n Diagram

Figure 6.31 plots the V-n diagram for the envelope of flight described by the RFP. The cruise speed is at Mach 0.8 at an altitude of 35,000 ft. The dynamic pressure limit, defined by the RFP, is 2,133 psf, which is a speed of Mach 2.47 at cruise altitude. The limit loads are determined to be +7 and -3 by the RFP as well with a safety factor of 1.5. The gusts are military transport winds of 66 fps at V_g, 50 fps at cruise speed, and 25 fps at dive speed. The gusts do not affect the size of the flight envelope for the aircraft being designed. The final flight envelope is shown in the figure by a bolded line.

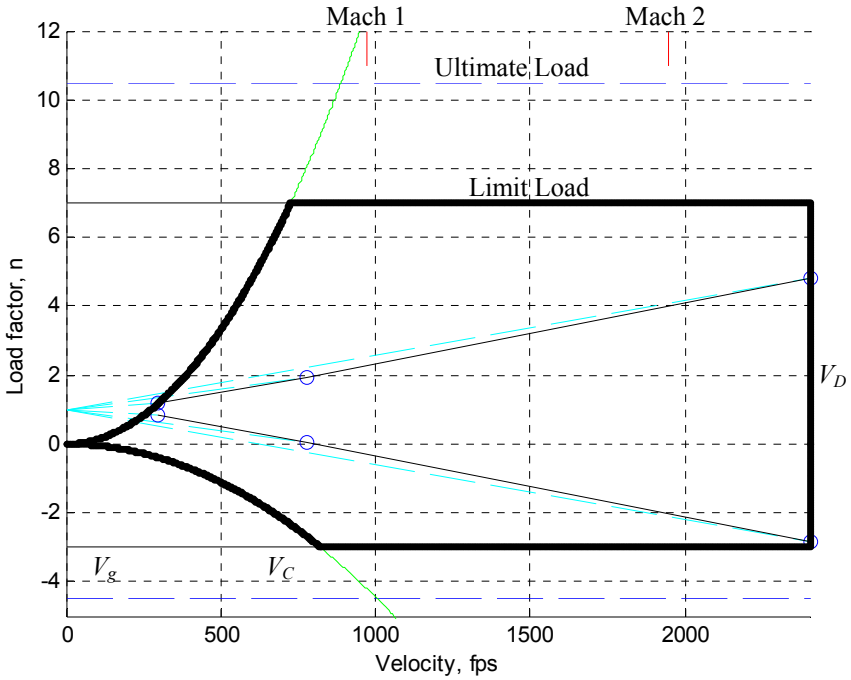

Figure 6.31: V-n Diagram

6.3. Design Structure

6.3.1. Fuselage

The forward fuselage consists of a honeycomb aramid skin, similar to the Raytheon Hawker Horizon design. The fuselage is supported by four aluminum lithium longeron beams. The lower longeron splits, to allow for the front landing gear to deploy. There are six bulkheads in the forward fuselage as shown in Foldout (2).

The design of having a wing, which can vary the sweep angle in mid flight, has been produced before. Over several aircraft types, including the F-14 Tomcat, the weight of the aircraft is increased greatly due to the increase of moving parts within them. The amount of shear and moment bending forces applied on the root of the wing varies as the sweep changes, resulting in a need for a strong structure. The conclusion drawn in the past is a strong wing box to handle such forces. In the F-14 Tomcat, the wing box is made of titanium in a vacuum with ion welding. With current technologies improving materials for components, the wing box of this design consists of a carbon-fiber frame, using the advanced RTM process. Also, the wing box can be further reduced by integrating it into the bulkhead structure, distributing the loads throughout the entire airframe. The integrated configuration can be seen in Figure 6.32. This will reduce the cost and weight of the airframe. The actuation system for the wing consists of a central hydraulic actuator that rotates a ball screw which in turn pushes or pulls a control rod along a track. When

the wings are in the unswept position, pressure forces will pull the wing forward. Therefore the actuator pulls the wing to keep it in place. The actuator movement can be seen in Figure 6.33. The mechanisms must be made out of titanium, due to the forces they experience and the complex shape of a screw needed. The ball crew system also allows only one actuator needed to control both wings, resulting in never experiencing a situation of differing leading edge angles. The middle fuselage contains six bulkheads (Foldout 2). The longerons are increased around the wing carry through box, allowing it to be smaller and even lighter as the loads are dispersed through the bulkheads. There are 4 longerons around the ducts to maintain their shape, which travel from the inlet to the end of the fuselage.

Figure 6.32: Wing carry through box: *(a) standing alone and (b) integrated into surrounding bulkhead sand longerons*

The aft fuselage is constructed similarly to the central fuselage with a few changes. The bulkheads are placed for support of the vertical and horizontal tails. Additional longerons are placed around the horizontal tail's pivot point due to the loads and stresses accumulated there. The engines are placed so that they can easily be removed via sliding out through the back, allowing for ease of repair and maintenance on the engines, while not breaking the bulkheads in the aft section and lowering their amount to four.

Figure 6.33: Ball actuator system as wing sweep mechanism

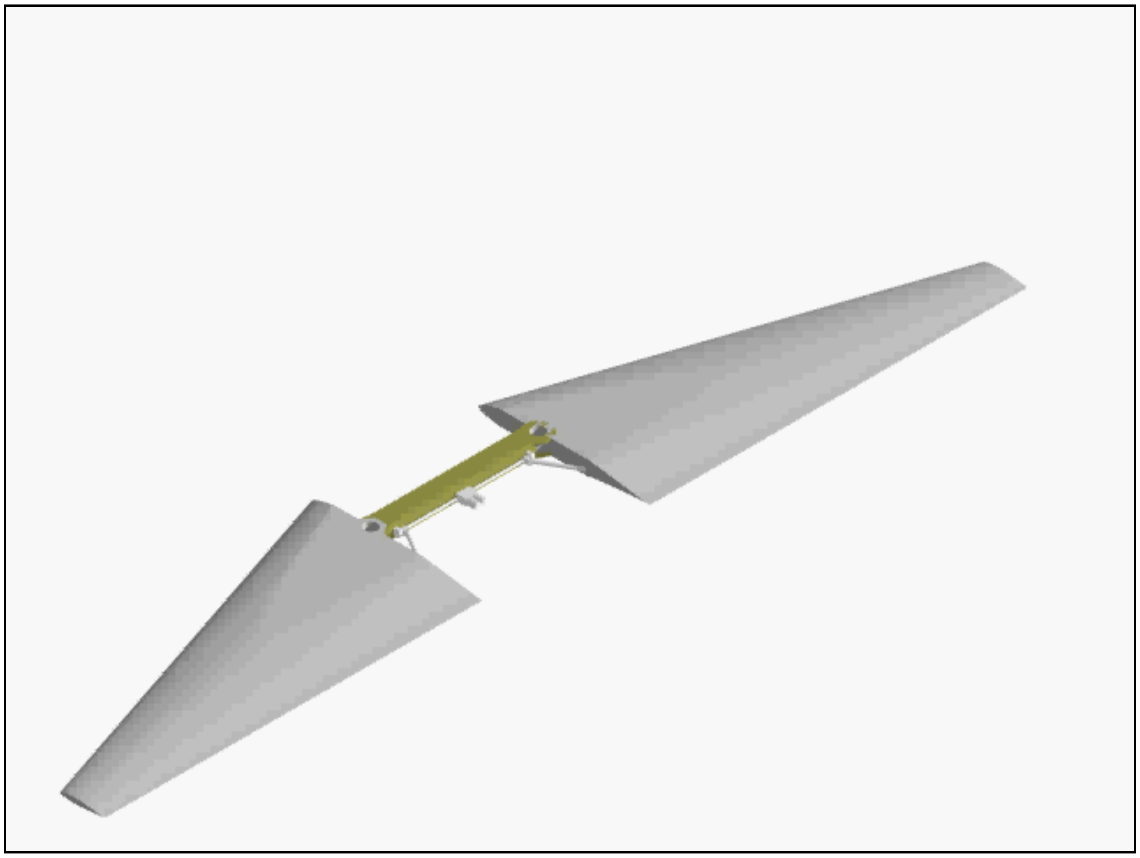

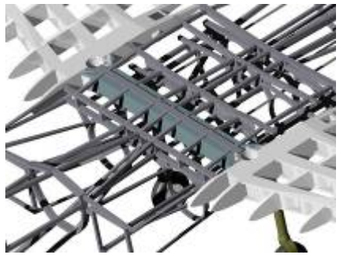

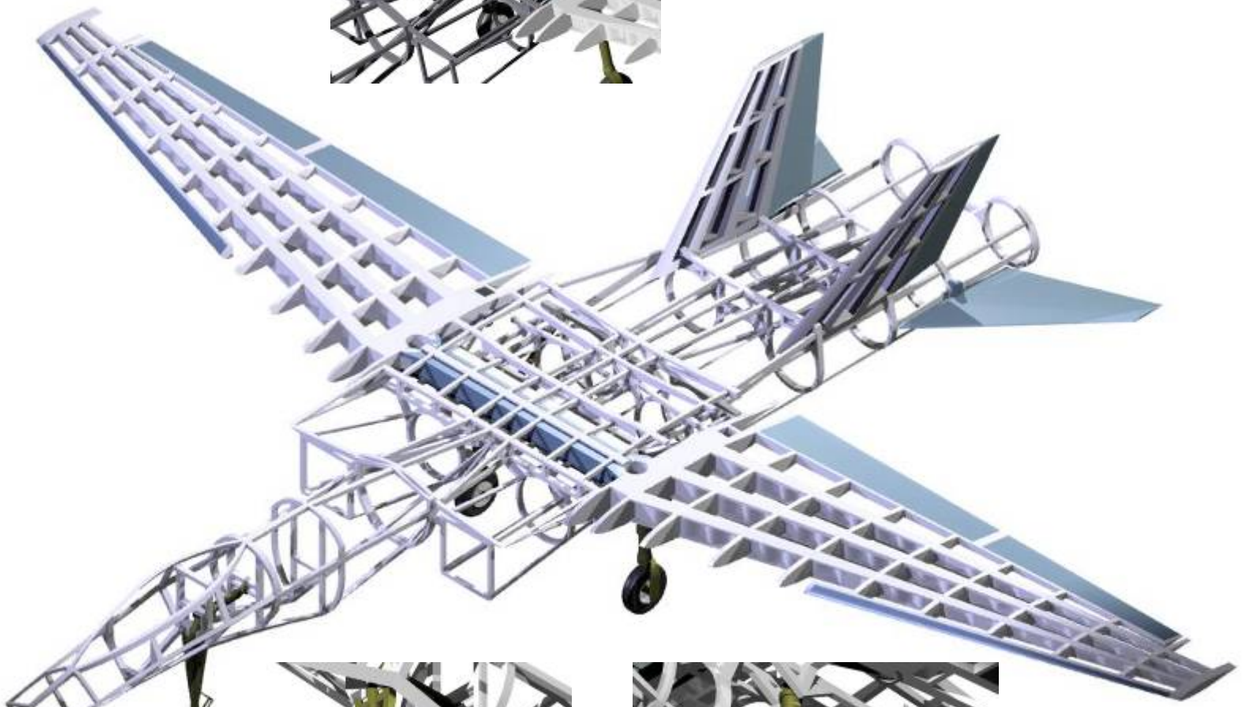

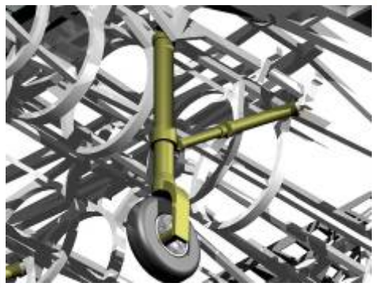

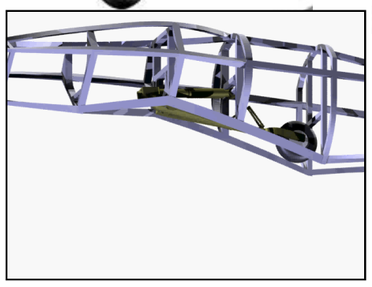

1 2 3 4 5 6 7 8 9 10 11 12 13 14 15 16

Bulkhead	Reason	Fuselage Station (in)
1	Nose support	54.00
2	Forward pressure bulkhead	84.00
3	Cockpit systems support	126.00
4	Front landing gear support	170.70
5	Front landing gear actuator support and aft pressure bulkhead	206.70
6	Vulcan cannon and FLIR mount	252.00
7	Inlet mount and support	313.00
8	Wing carry through box support	381.60
9	Wing carry through box mount and support	405.60
10	Wing carry through box and main landing gear support	431.80
11	Main landing gear actuator support	469.60
12	Main landing gear strut support	488.53
13	Vertical tail support	562.14
14	Vertical tail and engine support	614.70
15	Horizontal tail and engine support	655.90
16	Engine support	715.80

6.3.2. Wings

The wing structure has spars located at 20%, 40% and 60% of the chord length, comprised of new carbon-fiber composite using advanced RTM to produce. The induced stress placed on the wing, as in Figure 6.34.a shows the stress is concentrated on the pivot and actuator points, which results in usage of advanced composites and RTM at these points as well. Space is allotted between the spars and the control surfaces for electrical or mechanical parts associated with these. There are eleven ribs in the wing, ten of which are evenly spaced. The division of the first and second rib at the root of the wing is offset to support the reaction forces caused at the pivot point (see Figure 6.34.a Figure 6.35).

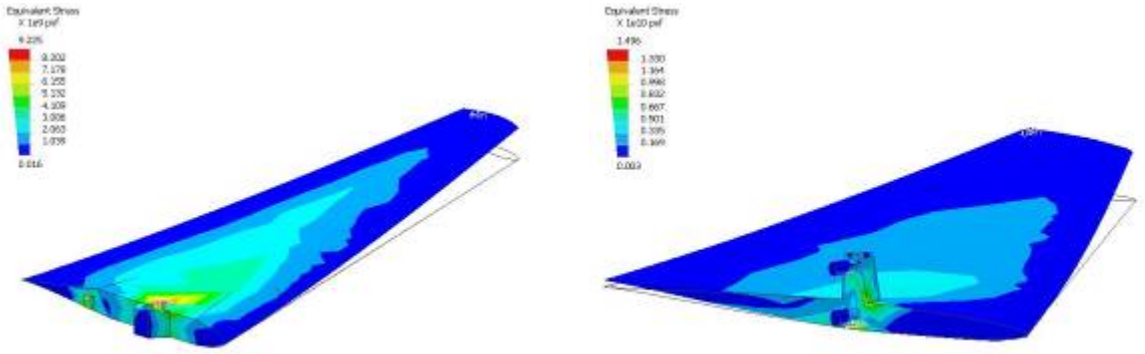

(a) Wing

(b) Horizontal Tail

Figure 6.34: Wing and Horizontal Tail stress analysis

The wing box contains sine wave beams as shown in Figure 6.35. The sine wave beam is difficult to construct from metals; however, with improving technology in composites, the task of creating these has become easier and more cost effective. A similar method has been applied to the F/A-22 Raptor, resulting in a reduction to the cost of the wing spars by 20% and decreasing the amount of reinforcement components to half the original.[17] A similar method is used on the design of this aircraft. The control surfaces will consist of all carbon fiber/epoxy components, which are becoming standard in most modern aircraft.

Figure 6.35: Wing structure with sine wave beams

6.3.3. Vertical Tail

The vertical tail(s) also contain aramid fiber reinforced skin, similar to the wings and fuselage. The spars are located on the leading edge and around the attachments to the bulkhead supports of the fuselage, which are located 20% and 65% of the chord respectively. The control surface is manufactured of a solid composite piece of carbon fiber/epoxy. Lockheed Martin has recently created a solid composite vertical tail for advanced fighter aircraft,[18] which has become more available in the future and will replace the current structure.

6.3.4. Horizontal Tail

The horizontal tail(s) is an all-flying tail, which consist of a solid piece of carbon fiber/epoxy and does not require the use of a trim tab or other deflective surfaces. All-flying horizontal tails are common amongst all modern fighter aircraft, since it allows more control in supersonic flight. More fibers are placed around the pivot point, which is located at 50% of the chord, due to a similar reaction as the wing experiences, shown in Figure 6.34.b. The linear actuator applies its force to the upper control arm to pivot the tail shown in Figure 6.36. The differential horizontal tails will move independently, allowing them to be used for creating additional rolling moment.

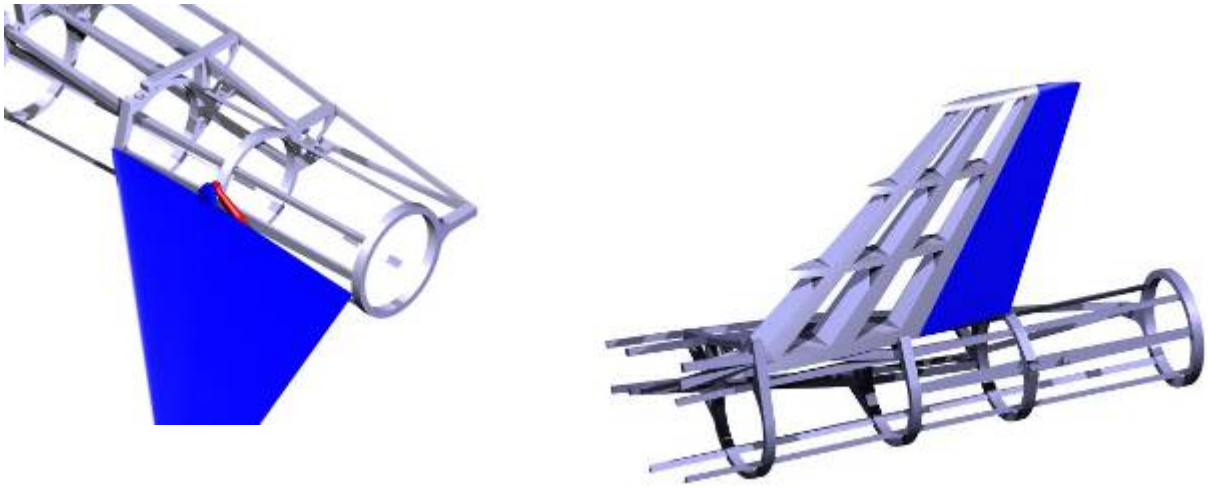

Figure 6.36 Horizontal and vertical tail structure setups: *Fuselage structure is only shown to centerline.*

6.4. Landing Gear

A tricycle landing gear layout is used for the *Shrike* interceptor and modeled after modern military aircraft. The main gear consists of two main struts incorporating a single wheel design. Due to volume constraints in the fuselage, the main gear was adapted to retract aft into the stowed position. The landing gear is made of a titanium alloy and shares the bulkhead around the wing carry through box to reduce the amount of material used in the aircraft. The space allotted to the wheel wells is optimized to allow for the expansion of the tire during takeoff, and also to allow cooling air to lower the temperature of the tire after retraction. The landing gear is attached to the aircraft at a height of 6.14 feet above the tarmac and 3.75 feet aft of the center of gravity. It is positioned to meet the tip-back and turnover angle requirements of 10 and 60 degrees respectively as shown in Foldout 1.[2]

The nose gear is a conventional strut-based, single wheel design that extends to its oleo maximum limit and locks into the stowed position upon retraction into the fuselage. The landing gear retraction was designed to accommodate both the placement of the FLIR and the Vulcan Cannon.

Oleo shock struts are incorporated onto the gear and are the most efficient dampening system. With excellent energy dissipation and good rebound control, the struts will absorb the high stresses associated with landing. Oleo-pneumatic shocks have an efficiency of 90% compared to 50 % for steel spring, 60% for rubber and 75-90% for oil/ liquid.[19]

Aircraft weighing less than 50,000 pounds are sufficiently supported by a single wheel per strut; therefore, the *Shrike* uses a single wheel per strut on both the main and nose gear. The *Shrike* is equipped with B.F. Goodrich New Design tires. New Design tires operate under higher internal pressures, which reduce their size and allow for higher landing speeds.[2]

The main gear tires have an outer diameter of 27.5", a width of 7.5", and a rim diameter of 16", while the nose gear tire measures 22" × 6.6"-10". Table 6.21 below shows the required and rated loadings of the tires.

Table 6.21: Landing Gear Tire Loading

	Required Load (lbs)	Rated Load (lbs)	Rated Pressure (psi)
Main Gear Tire	18,522	20,500	400
Nose Gear Tire	12,275	13,000	290

Carbon brakes are used on the main gear as opposed to steel because they dissipate heat more effectively and maintain higher brake efficiency during usage. Utilization of carbon brakes also reduces the weight and cost of maintenance for the design. An adaptive antiskid system is also incorporated to prevent the wheels from locking during operation on icy or wet pavement.

7. Weights

Weight is the most influential constraint on the cost of an aircraft. It was imperative to minimize the weight of the *Shrike* in order to meet the $15 million fly-a-away cost requirement. Methods of reducing the weight were mentioned earlier. To recap, weight has been reduced by:

- Utilizing advanced composite materials
- Utilizing new structure technologies (isogrid, sine wave beam, etc)
- Using Fly-by-light technology
- Use of Electro Hydrostatic Actuators
- Variable Sweep Wing

Initial weights were estimated using Daniel Raymer's[1] weight approximation for fighter aircraft. These approximations are summarized in Table 7.22. Each of the major components going into the *Shrike* was modeled in Autodesk's Inventor® Professional 10.[20] Inventor has the ability to apply material properties to the modeled parts and accurately calculate the physical properties of that part. Several parts can be combined and constrained in an assembly where the physical properties of the entire assembly can be calculated. Moreover, the constraints applied to these components allow them to interact with other parts and simulate the motion of actuators and dynamic systems of linkages. Once the major components had been modeled and assembled the final weight, CG and moments were determined by the program.

A comparison of the *Shrike* and the F-14 Tomcat (Table 7.22) especially shows how using EHAs and advanced materials techniques have reduced the weight of the *Shrike* compared to other wing sweep aircraft. The *Shrike* has a greater cost-to-weight ratio; however, the weight savings reap the benefit of a more cost effective aircraft.

Table 7.22 : Weight Comparison between the F-14 Tomcat and the *Shrike*

	F-14	*Shrike*
Empty Weight, lbs	40104	24000
Unit Cost, M$	38	53.7
Maximum TOGW, lbs	72900	43500
Cost Density, lbs/$	521.262	1057.471

7.1. Payload

Part of the government furnished equipment included the weapons carried by the HDI. The fold-out at the end of this section shows the breakdown of weight for the missiles (9M Sidewinder missiles and the 120M AMRAAM missiles) as well as the M61 A1 20 mm cannon ("Vulcan cannon") to be located on the aircraft.

7.2. Center of Gravity Location

The location of the center of gravity was initially found using the rough weight estimations for the wing, tails, fuselage, landing gear, and "all-else-empty" using Daniel Raymer's method outlined in his AIAA Aircraft Design handbook.[2] For the wing, tails and fuselage, weight estimations were determined by determining the density of each of the materials based on the volume that comprised that section of the fuselage in the model created in Autodesk Inventor. Figure 6.30 in the Structures sections summarizes the material composure of the wing, tails, and fuselage used to estimate the weight. The design of the fuselage was based on a Sears-Haack body with the volume estimated using a method described by Bud Nelson in his article "Design Scope for Student Supersonic Projects"[21] and the results of which are recorded in

Table 7.23. The volume estimate allowed an accurate fuselage to be modeled for the preliminary *Shrike* using the corresponding Sears-Haack body. Once the Fuselage was created the *Shrike* was filled with the components and the weights, and moments were generated.

Table 7.23: Preliminary Volume Estimation of *Shrike*

Component	Volume ft^3
cockpit	50.00
Avionics	365.00
AAR Radome	14.13
Vulcan Cannon	88.58
LDG	9.56
Hydraulic	19.74
Electrical	4.00
Environment	18.00
Aux Gear	2.00
Obogs/obiggs	2.00
WSM	140.82
Tail Carry-Through	85.85
Propulsion	20.00
Body	429.00
waste	140.71
fuel	352.77
TOTAL	1742.17

Table 24: Weights for the *Shrike* determined using a historical aircraft method

				CG			Moments of Inertia (Take Off)		
	Components	**Weight** lbs	**Mass** slugs	**X** ft	**Y** ft	**Z** ft	**Ixx** slug*ft²	**Iyy** slug*ft²	**Izz** slug*ft²
1	wing	2564.59	79.65	0.00	3.30	1.33	1768	3490	4288
2	H. tail	544.43	16.91	0.00	25.95	-0.66	11481	952	12418
3	V. tail	636.92	19.78	0.00	20.23	4.07	8686	526	8516
4	fuselage	6251.44	194.14	0.00	0.24	0.61	30745	2679	32811
5	Wingbox	2754.50	85.54						
6	main LDG	77.16	2.40	4.96	4.57	-0.47	177	64	233
7	nose LDG	328.94	10.22	-4.96	4.57	-0.47	342	258	588
	Structure	13157.97							
	engine mounts	63.21	1.96	~	~	~	~	~	~
	firewall	32.21	1.00	~	~	~	~	~	~
	engine section	32.92	1.02	~	~	~	~	~	~
	air induction	668.37	20.76	~	~	~	~	~	~
	engine cooling	258.95	8.04	~	~	~	~	~	~
	oil cooling	76.16	2.37	~	~	~	~	~	~
	engine controls	36.59	1.14	~	~	~	~	~	~
8	engine	2180.00	67.70	2.96	22.95	-0.64	36584	696	37150
8	engine	2180.00	67.70	-2.96	22.95	-0.64	36584	696	37150
	Propulsion	5528.41	**103.99**	**0.00**	**18.24**	**-0.64**			
9	Starter (APU)	100.00	3.11	0.00	22.42	-0.43	1564	1	1563
	Fuel and Tanks	739.73	22.97	~	~	~	~	~	~
	Flight controls	254.42	7.90	~	~	~	~	~	~
	instruments	150.96	4.69	~	~	~	~	~	~
	Hydraulics	131.29	4.08	~	~	~	~	~	~
10	Pump 1	85.23	2.65	4.49	17.66	-0.26	826	54	879
10	Pump 2	85.23	2.65	-4.49	17.66	-0.26	826	54	879
11	Reservoir (MG)	64.40	2.00	-5.00	1.27	0.74	5	51	54
12	Reservoir (NG)	64.40	2.00	0.00	-15.83	0.93	503	2	501
	Electrical	300.00	9.32	~	~	~	~	~	~
13	Generator 1	56.39	1.75	-4.50	19.16	-0.02	643	36	679
13	Generator 2	56.39	1.75	4.50	19.16	-0.02	643	36	679
14	Avionics	1101.11	34.20	0.00	-34.33	2.45	40513	217	40314
	AAR	450.00	13.98	0.00	-26.91	0.52	10137	10	10133
15	Furnishings	250.00	7.76	0.00	-22.83	0.74	4050	4	4046
	A/C and anti-ice	203.82	6.33	~	~	~	~	~	~
	Handling gear	13.32	0.41	~	~	~	~	~	~
	Systems	4171.09	**129.12**	**0.00**	**19.34**	**-0.23**	**48316**	**7**	**48309**
16a	AMRAAM	326.00	10.12	0.00	2.69	-0.26	179	1	178
16b	AMRAAM	327.00	10.16	0.00	15.69	-1.26	2620	17	2604
17	Sidewinder	190.00	5.90	-3.00	6.69	-2.51	343	90	359
18	Sidewinder	191.00	5.93	3.00	6.69	-2.51	344	91	360
19	Vulcan Cannon	275.00	8.54	0.00	-17.00	0.00	2470	15	2470
20	Ammo Drum	300.00	9.32	0.00	-12.83	1.28	1553	21	1539
	Weapons	1609.00	**49.97**	**0.00**	**2.96**	**-1.11**			
21	Fore Tank 1	6420.33	199.39	0.00	-6.55	1.22	10936	775	10905
22	Inboard Wing	3553.49	110.36	15.00	11.28	-0.62	14481	44042	58420
23	Outboard Wing	2455.86	76.27	30.00	17.20	1.35	22905	111452	134068
24	Aft Tank 1	1754.19	54.48	0.00	7.70	0.62	3534	180	3647
25	Aft Tank 2	3207.66	99.62	0.00	14.61	0.56	21758	298	21910
26	Aft Tank 3	2155.15	66.93	0.00	21.17	-0.18	30290	123	30360
	Fuel	19546.68	**607.04**	**0.54**	**0.53**	**0.04**			
	TOTAL	**Weight** lbs	**Mass** slugs	**X** ft	**Y** ft	**Z** ft	**Ixx** slug*ft²	**Iyy** slug*ft²	**Izz** slug*ft²
27	*take-off*	**44013**	**1367**	**0.01**	**33.83**	**0.67**	**280322**	**166846**	**442496**
28	*landing*	**26560**	**1963**	**0.00**	**30.59**	**0.50**	**193075**	**10014**	**199835**

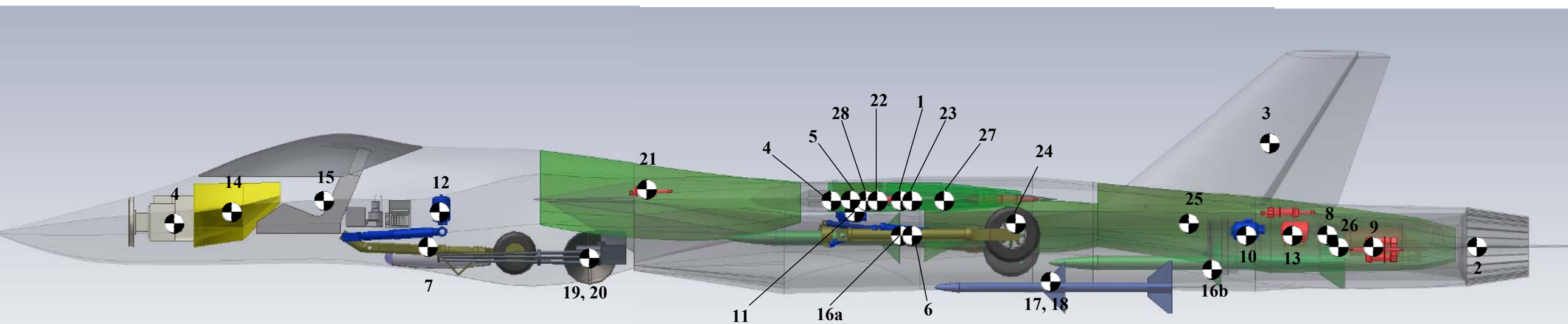

8. Systems and Avionics

The *Shrike* is proposed as a manned vehicle. Unmanned vehicles are susceptible to jamming and interference from electromagnetic emissions. Granted there are means to appropriately shield the critical elements in the system, and their added weight would be negated by the systems that could be reduced in size or removed by the removal of a pilot. Remarkable progress has been made in the realm of UCAV's; however, expectation has arisen to have "one-third of the deep-strike force with unmanned aircraft by 2010."[22] The technology to make such a vehicle possible is still being developed and has not yet been proven reliable for such missions and is expected to play more of a reconnaissance role. This role will not likely expand until much further after the creation of the *Shrike*. The majority of Americans will feel safer knowing that there is another American flying an interceptor overhead than if it were an artificial intelligence. Additionally, the interceptor's missions will be host over friendly territory, where the pilot will have the advantage over a foreign strike and the risk of human losses will be much less than if the offense was being run over foreign soil. Moreover, the missions that will be flown by this vehicle will not be particularly weary to the pilot, especially with the installation of an autopilot for the four hour loiter.

8.1. Major Systems

8.1.1. Avionics

An autopilot feature is installed in the *Shrike* to reduce pilot weariness during the long loiter phase of the DCAP mission. A FLIR camera is mounted below the cockpit and next to the cannon in order to enhance the pilot acquisition of targets through poor visibility conditions. A vehicle management system will be programmed with special logic for the wing to sweep as the aircraft accelerates towards the speed of sound, at which point the wings will be completely swept back. A navigation, communication and identification (ICNIA) system will be a part of the *Shrike's* avionics package as well.

8.1.2. Flight Control

The Shrike is designed to be a More Electric Aircraft (MEA) by integrating EHAs into its flight controls. EHA's are used to deflect all of the *Shrike*'s control surfaces. Motors controlling the rudders, elevators, and ailerons will be deflected using EHA's that will need to me powered by integrated drive generators. Power is sent where it is needed via a power distribution assembly while secondary power assemblies further control power flow to less critical systems. The control surfaces on the proposed aircraft will be deflected using EHA's while landing gear,

missile ejections and wing sweep will be operated via hydraulic systems. Refer Figure 8.37 and Figure 8.38 for the details on the setup of these systems. The power lines and optic lines will be quadruply redundant with four flight control computers coordinating the *Shrike's* movement. There needs to be a breakthrough in electromechanical actuator technology before a completely electric aircraft can be created. Currently, EMAs generate a tremendous amount of heat that cannot be tolerated within an aircraft. However, EMAs are much more responsive and lighter than EHAs. [23]

Fly-by-light technology will be used in the proposed HDI because it is invulnerable to electromagnetic interference, decreasing the amount of shielding needed for wiring. A digital FBL system can handle more information faster than its FBW counterpart as well. Replacing wiring with fiber-optic cables alone would reduce weight. FBL is capable of handling more data faster than FBW systems. Overall FBL systems can reduce weight by approximately 25%, volume by about 30%, cooling by nearly 40%, and cost by about 25%.[24]

Full Authority Digital Engine Control (FADEC) controls the engines fuel flow as well as monitoring the engines performance. The FADEC ensure better fuel efficiency, does not allow unnecessary stress on the engine, fail safe with levels of redundancy built-in, extends the life of the engine, and can operate to compensate for emergencies.[25]

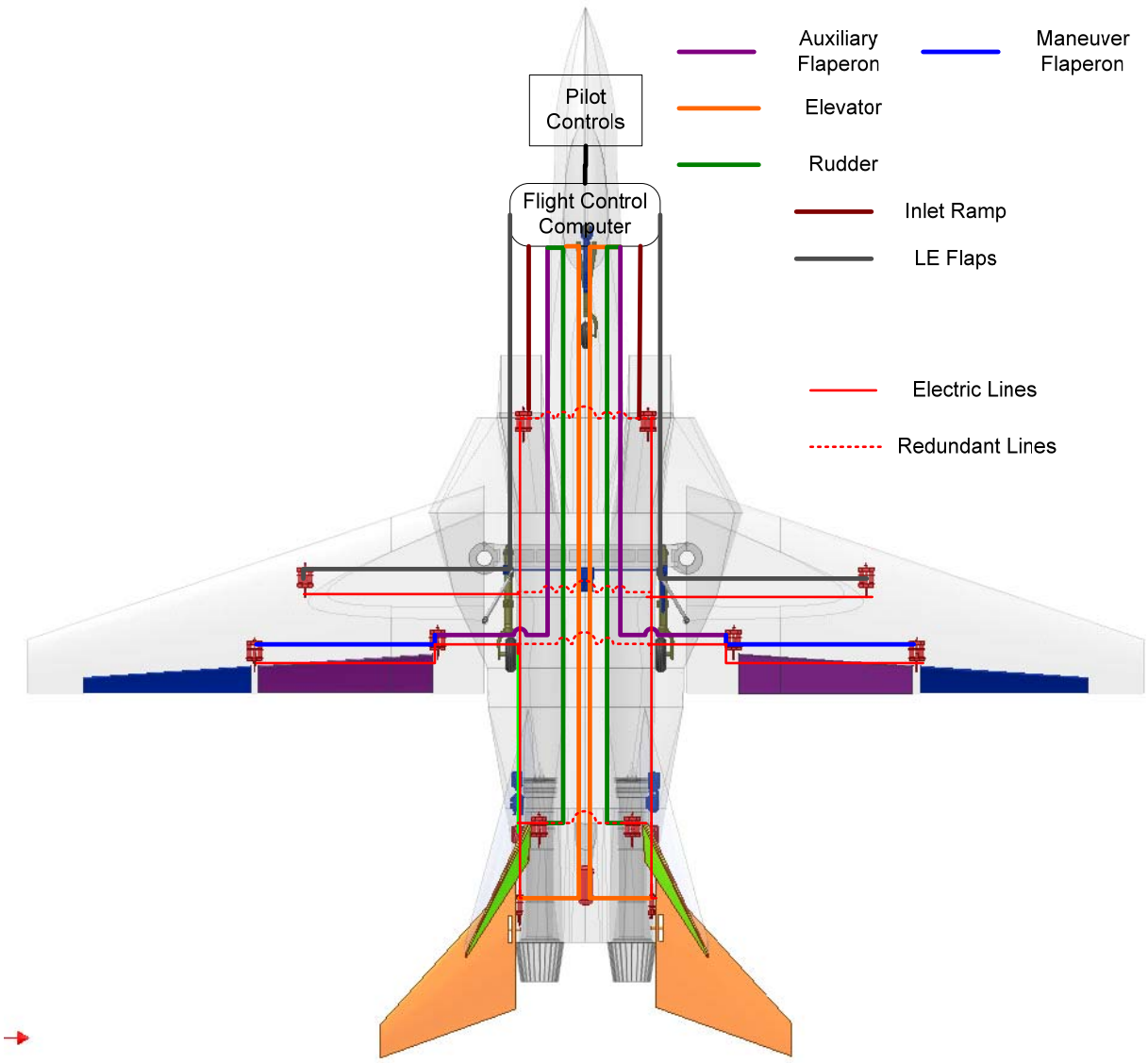

Figure 8.37: Flight Controls with Electrical Wiring and Fiber Optic Connections

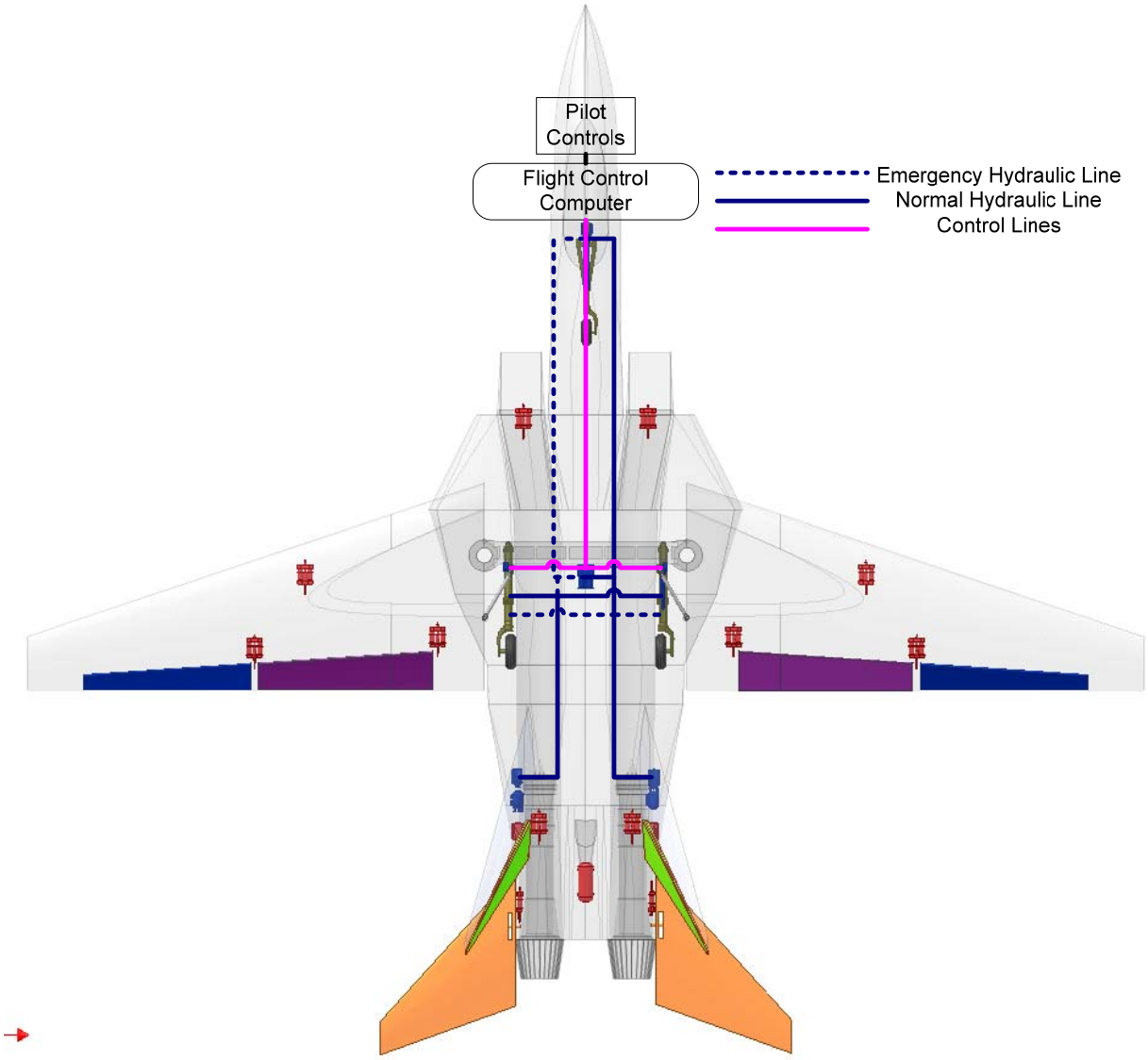

Figure 8.38: Fight Controls with Hydraulic Connections and fiber optic control lines

8.1.3. Hydraulic system

Hydraulic systems are heavier than electro-hydrostatic actuators (EHA's) but are less susceptible to failure. Such a system also requires routine maintenance. Despite these disadvantages, the *Shrike* will require a hydraulic system to operate at the loads expected to after the variable sweeping of the wing. The hydraulic ball screw actuator to push the wing into its unswept position will ensure that any hydraulic failure will allow the wing to remain in its position until the aircraft is able to land rather than move freely about the pivot and possibly ending in disaster. The *Shrike* will feature two hydraulic pumps used to actuate the wing sweep and to power the nose and main landing

gear. Since the hydraulic system will not be used throughout the aircraft it does not need to be as large of a system normally used to power a fully hydraulic aircraft. Maintenance and cost of the aircraft will be reduced by incorporating proven hydraulics rated at 4000 psi. While heavier and greater in volume than a developing 8,000 psi system, the limited use of hydraulics in the *Shrike* justifies the exchange of small savings in weight and volume for reliability and low maintenance.

There is a hydraulic pump connect to each engine. Figure 8.38 shows how the hydraulic power is routed to the landing gear and ball screw actuator. The right hydraulic pump services the wing sweep mechanism (WSM) and the nose gear, but also has emergency lines running to the main gear. Likewise, the left hydraulic pump has lines running to the main gear with emergency line running to the WSM and nose gear.

8.1.4. Electrical system

A schematic of the electric power distribution is described by Figure 8.37. The electric lines are run so that the integrated drive generators (IDGs) on the left and right service their respectively side of the aircraft. Electric lines are linked with redundant lines in the case of a failure of one the generators.

EHAs with a variable speed electric motor (Figure 8.39) enable the motor to shut off when the actuator is not needed. The other version of the EHA has a variable displacement swash plate with a constant speed electric motor.

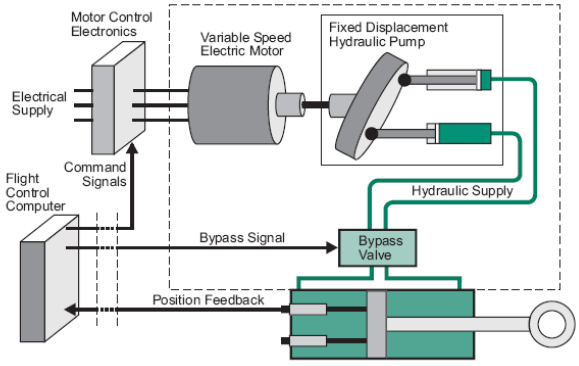

Figure 8.39: Schematic of an EHA with a Variable Speed Electric Motor
(Courtesy TRW Aeronautical Systems)

Hydraulics and Electric systems require 50 kW of power. Since our engine can produce 225 kW of maximum power there will be no worry over the supplication of power. Moreover, at wind milling speeds integrated electric generators produce 25 kW of emergency power.

8.1.5. Fuel System

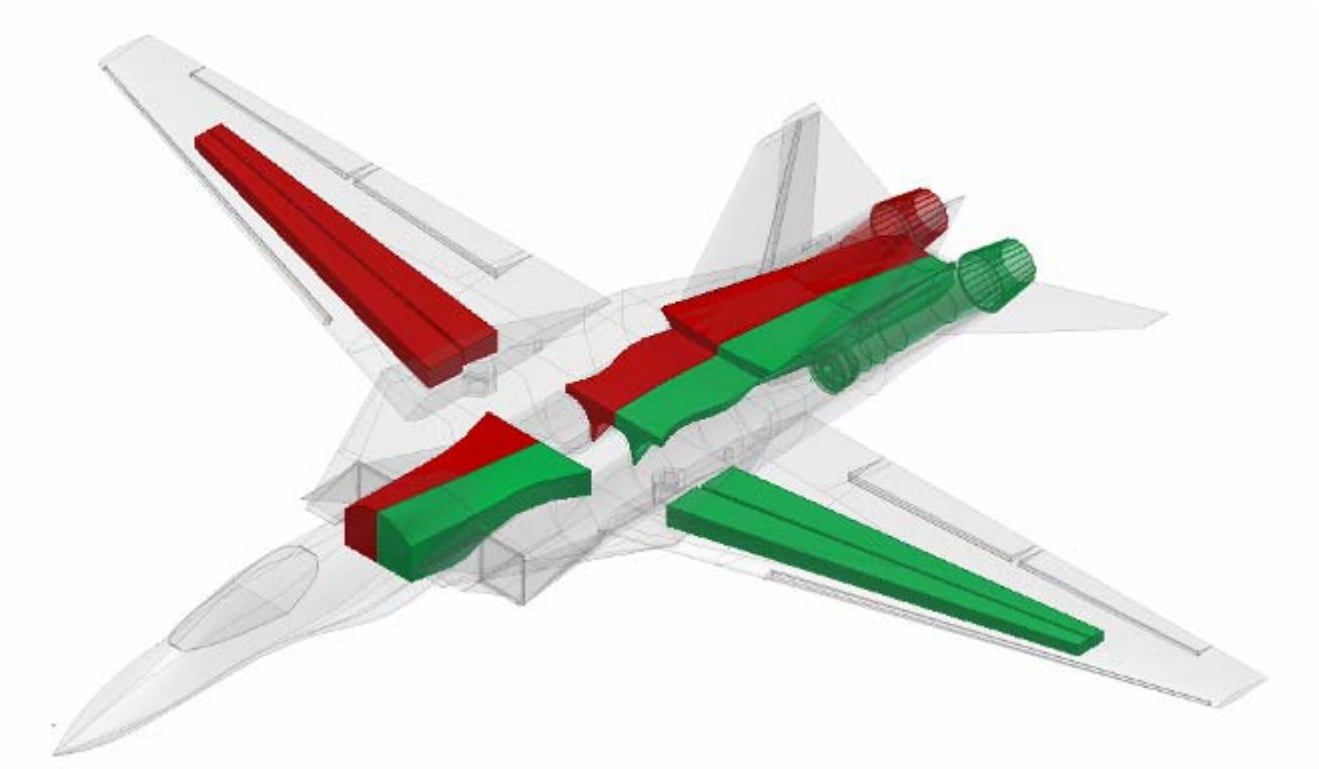

Figure 8.40: Fuel Tanks – Right Engine Feed (red), Left Engine Feed (green)

The fuel needed to complete the missions described in the RFP. Conformable tanks have been researched and considered for extra fuel storage during the four hour loiter mission, however, during that same mission the *Shrike* must also dash at mach 2.2 for 100 nm. At supersonic speeds a conformable tank will add tremendous drag, reducing the maximum Mach number. Therefore, great pains were taken to fit the entirety of the *Shrike's* fuel within the body.

The RFP requires that all of the tanks be self-sealing, so rubber bladders line the integral fuel tanks. A shot passing through the tank would then reseal because of the membrane. Refueling will be through valves on both wing tanks. Air refueling is not necessary because there is no need for a HDI to refuel in the air when friendly airports are abundant. Fuel tanks feeding the left and right engines are connected so that in the event of an engine failure, fuel can be fed to the remaining engine from the other engine's tanks. The fuel needed per mission is available in Table 8.25: Fuel Needed per Specific Mission.

Table 8.25: Fuel Needed per Specific Mission

Mission	Fuel Needed, lbs
DCAP	17681
PDI	5450
I/E	15616
* I/E has a maximum dash range of 5200 nm dash to the aircraft to escort	

8.2. Other Systems

8.2.1. Cockpit Layout

The canopy is a single clear piece of monolithic polycarbonate hinged behind the pilot. No additional structures are used in the canopy allowing the pilot to have unsurpassed visibility in all directions. This yields a great advantage to the pilot in a turning dogfight, and especially at high speeds where relying on visible cues is more acceptable to pilots.

The cockpit will utilize a Multi-Function Display System (MFDS) with panoramic view capabilities. The system is developed by Rockwell Collins and incorporates an 8" by 20" Liquid Crystal Display (LCD) located in the middle of the consol as the primary display. One main image and up to six smaller full motion images can be shown on the LCD screen which is run by one-gigabyte-per-second data interfaces. Using touch screen features the MFDS can easily be preprogrammed and reconfigured for different missions and missions segments. Engine data, hydraulic systems, information on control devices, communications and all other systems and subsystems can be viewed on any of the small screens or main LCD. A control pad, and configuration screen are located directly below the main LCD to help the images. The multitude of displays in one area along with touch screen capabilities increase pilot situational awareness while reducing work load. LCD screens eliminate the need for numerous small glass dial gauges that used to be used to manage aircraft systems. All of this can be provided in high-luminance, high-contrast, and high-resolution picture with no viewing angle effect.

The *Shrike* will use a Heads-Up-Display (HUD) developed by Vision Systems International. The HUD provides the pilot with altitude, heading, airspeed, bank angle along with enemy tracking information. Information is projected onto a screen above the main LCD and in the line of sight of the pilot. Night vision and infrared technologies are integrated into the HUD providing all weather capabilities for the pilot.

The control stick is located on the right side of the aircraft while the throttles are located on the left side – both of which can be seen in

Figure 8.41. The stick is pressure sensitive and does not require the large displacements of older center stick controls. Buttons on the control stick allow the pilot to manage the weapons, trim and navigation systems without removing a hand from the throttle or control stick. The throttle is located on the left side of the cockpit and controls engine settings, speed brakes, and along with radio communications. Two throttles are linked together as one but can be controlled separately if an engine is out or if different throttle settings are required. An ACES-II ejection seat will be utilized because of its proven reliability in current United States fighters. The seat consists of the seat casing, control-electronics, a container to hold the pilots parachute, survival kit assembly, emergency oxygen assembly and the ejection mechanism. It is a zero-zero seat having the capability to eject at zero flight speed. The right arm of the seat has been modified so the pilots arm can rest in it while controlling the aircraft. This modification requires no extra manufacturing as it is used on the current F-16 aircraft[26].

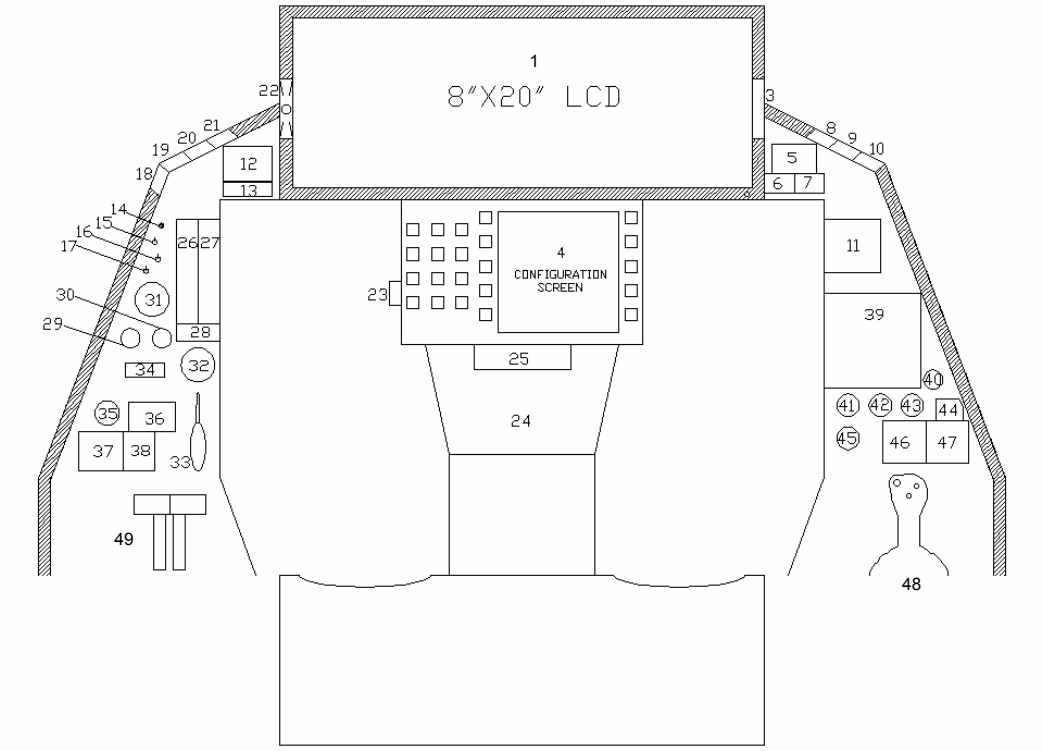

1	8''X20'' Liquid Crystal Display with Multiple Windows	26	Fuel Flow Indicators
2	Heads-Up-Display (not pictured)	27	Thrust Indicators
3	Air Refuel Status/NWS Indicator	28	Digital RPMs Readouts
4	LCD and HUD Control Pad and Screen	29	Left Engine Oil Pressure Indicator
5	Attitude Indicator	30	Right Engine Oil Pressure Indicator
6	Digital Airspeed Indicator	31	Nozzle Position Indicator
7	Digital Altimeter	32	Fuel Quantity Indicator
8	Dual FC Fail Warning Light (Red)	33	Landing Gear Control Lever
9	Hydraulic Pressure Warning Light (Red)	34	Parking Break Lever
10	Canopy Warning Light (Red)	35	Jettison Button and Selector
11	Vertical Velocity Indicator	36	Canopy Jettison Control Panel
12	Compass and Threat Warning Indicator	37	Auxiliary Weapon Switches
13	Autopilot Switches	38	Canopy Controls
14	IFF Identification Button	39	Caution Light Panel
15	SMS Power Switch	40	Oxygen Flow Indicator (Blinker)
16	Alternate Release Button	41	Starboard Hydraulic Pressure Indicator
17	Master Arm Switch	42	Port Hydraulic Pressure Indicator
18	Left Engine Fire Warning Light (Red)	43	EPU Fuel Quantity Indicator
19	Right Engine Fire Warning Light (Red)	44	Cabin Pressure Altitude Indicator
20	Takeoff/Landing Configuration Warning Light (Red)	45	Liquid Oxygen Quantity Indicator
21	Master Caution Light (Amber)	46	Starboard Electrical Indicator and Switches
22	Angle of Attack Indicator	47	Port Electrical Indicator and Switches
23	Rudder Pedal Adjustment Knob	48	Side Stick Controller
24	Communication Control Panel and Buttons	49	Throttle Controller
25	UHF Channel/Frequency Indicator		

Figure 8.41: Schematic of Cockpit Layout

8.2.2. Fire Control Systems

The IRSTS will detect and track an enemy jet aircraft by sensing the infrared radiation it gives off. Compared to its radar counterpart, the infrared tracking has less range and is affected by weather.

The active array radar can sense aircraft in any direction, whereas traditional radar antennas must make two passes to confirm the position of an object. Active array in conjunction with the aircraft's computing system may track multiple targets, sense short and long range objects, and communicate with missiles. Weather will not affect the radar array.

8.2.3. Equipment

Other equipment placed in the aircraft, and vital to a manned operation of the aircraft, are the OBOGS, OBIGGS, APU, and the ejection seat. Two percent of the mass flow from the engine is used to drive the environmental systems (OBOGS and OBIGGS). The APU may be turned on in situations where perhaps one of the IDGs fails and a certain amount of extra power is needed to land the aircraft or complete the mission.

8.2.4. Countermeasures

The INEWS supplied by the government for the HDI will be utilized for the purpose of detecting, correlating, and identifying threats and act automatically react by using countermeasures (chaff and/or flares) to effectively neutralize imminent threats.

8.2.5. Anti-Ice Systems

Since the *Shrike* is already design for electric power, Thermion fabric can be placed in the wings in upper, lower, leading edge, and parting breaker strips. This process of anti ice reduces power consumption, overall, and is lighter in weight than the bleed air method traditionally used.[27]

8.3. Weapons

The missiles carried by the *Shrike* will be semi-submerged within the fuselage. In this configuration the missiles will not add nearly as much drag as if they were on pylons and they will not consume a large amount of volume in the fuselage. The cannon is placed close to the centerline of the aircraft and it is out of view of the pilot and the engine inlet.

Figure 8.42: AIM 7 "Sparrow" Missile semi-submerged in F-14 fuselage[28]

8.3.1. M61A1 20 mm "Vulcan" cannon

Figure 8.43: M61A1 20 mm "Vulcan" Cannon

The M61A1 20 mm cannon is a Gatling gun with six barrels firing once per revolution giving the cannon a 100 rps rate of fire. Since there are six barrels on the gun, weapon life is drastically increase as erosion and heat generation are minimize. Jams occur at a rate of once every 10,000 firings. The barrels are rotated by an electric motor. To prevent sudden yawing motion, the cannon must be located near the centerline of the fuselage.

8.3.2. AIM – 9M "Sidewinder" Missile

Figure 8.44: AIM – 9M "Sidewinder" Missile

The Sidewinder is an air-to-air missile used for its short range heat-seeking ability; however, in order for it to track a target the pilot must maintain a lock on the enemy aircraft. The missile is launched from a rail as well, so it requires a line of sight to the target in front of the aircraft.

8.3.3. AIM – 120 AMRAAM

Figure 8.45: AIM – 120 AMRAAM

The AMRAAM is an all-weather, beyond –visual-range missile. It has an active radar, inertial reference unit and microcomputer to make it somewhat independent of the fire control system onboard its parent aircraft. These missiles allow the pilot a greater freedom to maneuver in combat as when one is fired, the pilot does not need to maintain a radar lock.[29] Figure 8.46 below shows the weapon loading combinations and locations of Sidewinder and AMRAAM missiles onto the *Shrike*.

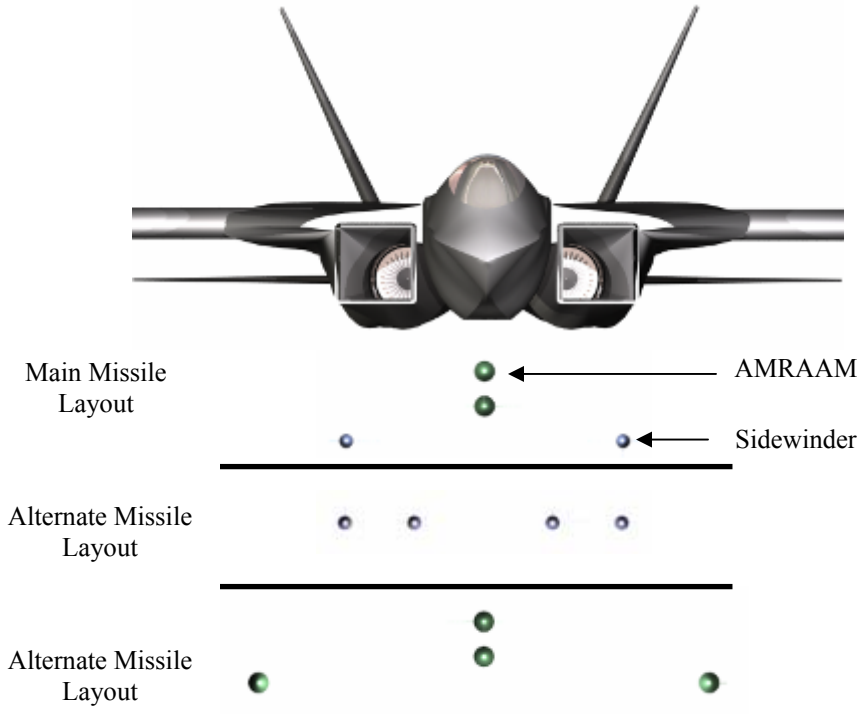

Figure 8.46: Various Missile Loading Configurations

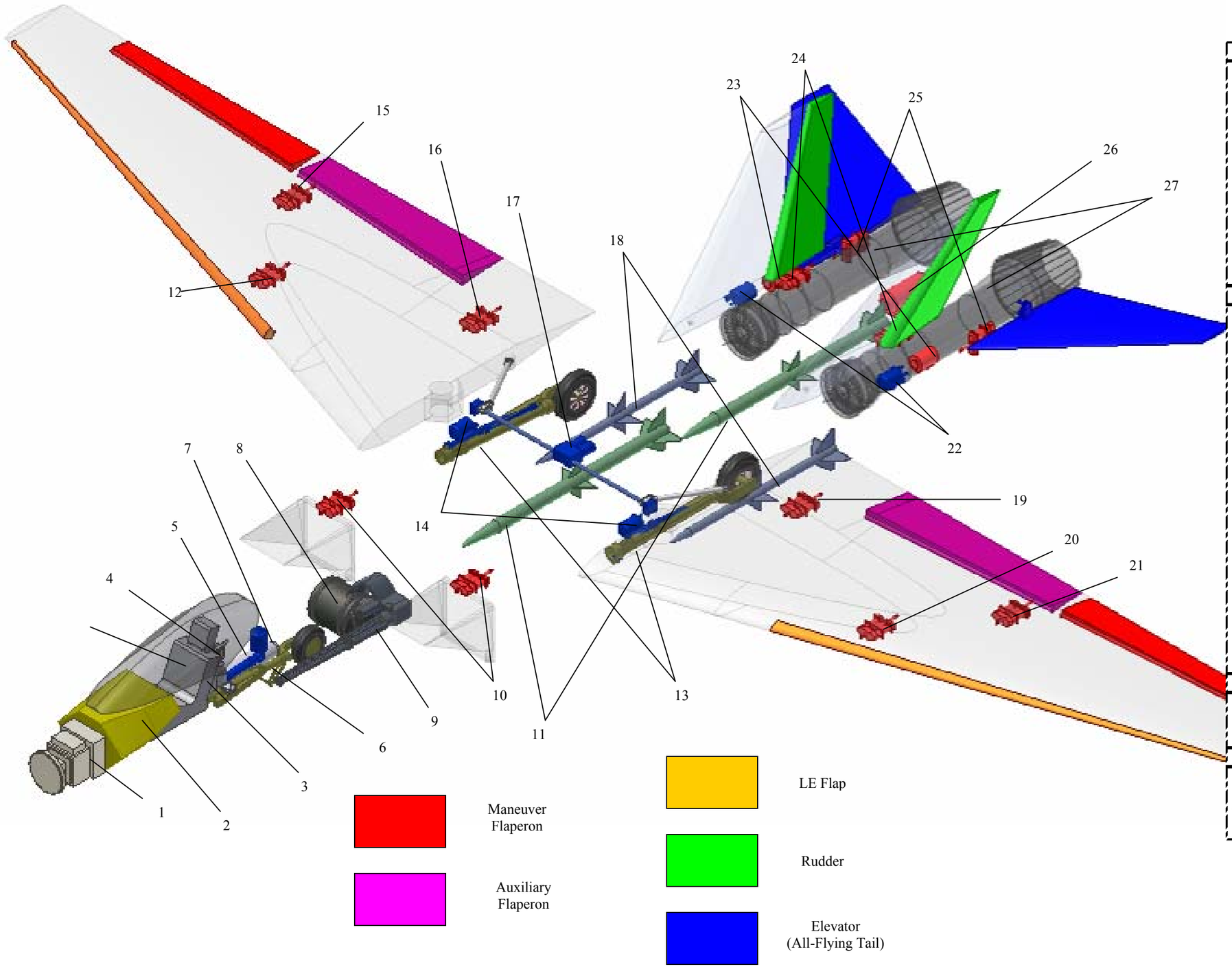

Avionics	
Base Suite	
ICNIA	2
MFDs	2
HUDs	2
Data Bus	2
ECM Equipment	
INEWS	2
Flight Propulsion Control System	
Vehicle Management System	2
Fire Control Systems	
IRSTS	2
Active Array Radar	1
Systems and Equipment	
Hydraulics	
Ball Screw Actuator	17
Hydraulic Generator	22
Reservoir	7, 14
Electrical System	
Electrical Generator	24
Maneuver Flaperon EHA	15, 21
Auxiliary Flaperon EHA	16, 19
LE Flap EHA	12, 20
Rudder EHA	24
Elevator EHA	25
Inlet Ramp EHA	
Other Systems/Equipment	
Ejection Seat	3
OBOGS	4
OBIGGS	4
FLIR	5
Landing Gear	
Nose	6
Main	13
Propulsion	
Engine (RR EJ200)	27
APU	26
Weapons	
AMRAAM	11
Sidewinder	18
Vulcan Cannon	9
Ammo Drum	8

Figure 8.47: The *Shrike's* system layout

9. Cost Analysis

Cost is a very important criterion for any military/government program – often the deciding factor. One of the primary aspects of the RFP is the requirement that pertains to the cost of the aircraft. The RFP states that the flyaway cost is to be estimated for the production of 1000 units and that each aircraft produced should not exceed $15 million in 2006 $US.

The unit cost also known as life cycle cost is broken down into the following components: flyaway, Research Development Test and Evaluation (RDT&E), acquisition, operation / maintenance, and profit costs. The equations used to estimate cost analysis are outlined in *Airplane Design: Part VIII* by Roskam[30], *Design of Aircraft* by Thomas Corke[31], and *Aircraft Design: A Conceptual Approach 3rd Edition* by Raymer.[1] The cost analysis takes into account the complexity of the structure, the materials used, and the overall weight of the aircraft. Cost estimations used throughout the analysis are based on 2006 $US value.[32]

9.1. Flyaway Cost

The flyaway cost is dependent upon the airframe, engine, and avionics. The government furnished equipment (avionics cost) were estimated to be $2.5 million. The two Rolls Royce engines were estimated to be approximately $7.02 million. The total flyaway cost for 1000 aircrafts per aircraft is $16.14 million. The flyaway cost breakdowns are shown in Table 9.26: Flyaway cost analysis. Total flyaway cost analysis was also done for 100, 500 units. A learning curve graph can be seen in Figure 9.48 where we can note that for the production of 100 units the flyaway cost will be $44.1 million, for 500 units it will be $19.9 million, and for 1000 units it will be $16.14 million.

9.2. Research, Development, Test and Evaluation Cost

The RDT&E cost includes most of the initial steps in the aircraft development process. The multiple elements in which RDT&E is derived from include: the airframe engineering hours, development support, profit, and finally the number of flight test aircraft to include – engine and avionics, labor, materials, tooling, and quality control. The cost variables used to calculate RDT&E and acquisition cost are shown in Table 9.27. The total cost of RDT&E is in Table 9.28.

9.3. Acquisition Cost

The acquisition phase refers to the fabrication of production aircraft, *Q*. Table 9.27: Cost variables, was used to determine the acquisition factors. The elements used in the derivation of the acquisition cost (Table 9.29) are: engine and avionics, labor, materials, airframe engineering hours, tooling, quality control, and tooling.

Table 9.26: Flyaway cost analysis

Avionics	$2,500,000
Actuator	$750,000
Propulsion	$7,020,000
Structures	$5,870,000
TOTAL Flyaway	**$16,140,000**

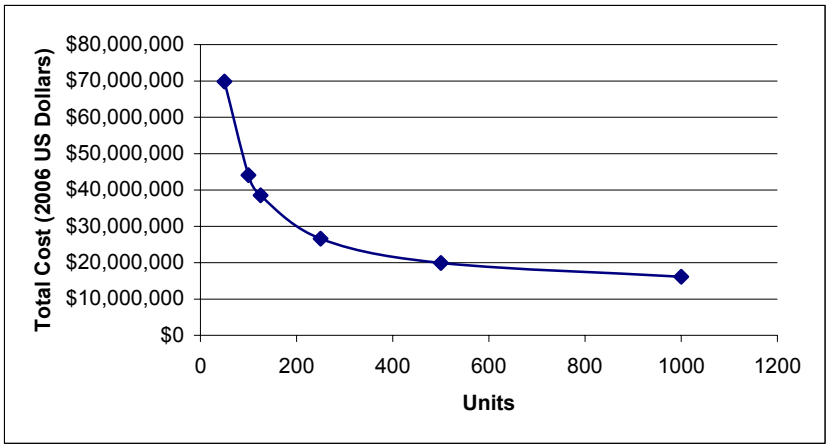

Figure 9.48: Learning Curve for Flyaway with Dependence upon Units

Table 9.27: Cost Variables

Empty Weight	22000
Max. Velocity	2456.16
Q	1000
Flight test	3
N_eng	2000
Thrust Max.	20196
Max Mach	2.2
Turbine inlet temp	2700
Avionics	2510000

Table 9.28: Total RDT&E cost analysis

sub-TOTAL	$5,704,992,844.00
Profit	$570,499,284.40
Total RDT&E	$6,275,492,129.00

Table 9.29: Total Acquisition cost for 1000 aircrafts

Airframe Manufacturing	$4,762,881,068
Tooling	$2,553,770,592
Labor	$10,427,698,469
Materials	$5,079,730,292
Engine	$7,270,000
Quality Control	$1,538,871,173
Profit	$2,437,022,159
TOTAL Acquisition	$26,807,243,753

9.4. Operation and Maintenance Cost

The main O&M costs are fuel, lubricants and maintenance. The average fighter aircraft is flown 300-500 hours per year. In order to get the estimate of yearly fuel usage a mission is selected and the total duration and the amount of fuel consumed is then used to determine the average fuel burned per hour. This value is then multiplied by the average yearly flight hours per aircraft. Finally, the total amount of fuel used per year is multiplied by the fuel price which is $3.70 per gallon (2006). The *Shrike* has a maximum capacity of 2,663.143 gallons per flight. Oil cost can be neglected since it is assumed that oil cost averages lower than half a percent of fuel cost.

Scheduled maintenance is done on most military fighter aircraft every 100 hours of flight and necessitates 10-15 hours of maintenance for every hour of flight; the cost of maintenance is $86 hourly. Although the *Shrike* is a variable sweep aircraft, it requires minimal maintenance because it is primarily composed of composite materials and utilizes fly-by-light technology. Table 9.30 shows the total cost of fuel and maintenance required per year depending on the hours of flight.

Table 9.30: Fuel and Maintenance required per year

OPERATION & MAINTENANCE		US $ (2006)
300 hours	fuel	$2,924,250.12
500 hours		$4,866,443.24
3 X 100 hr inspection	maintenance hrs/flight hr	$3,096,000.00
5 X 100 hr inspection		$5,160,000.00
sub-TOTAL OP/MAINT		$6,020,250.12
profit (3 X 100 hr inspection)		$602,025.01
profit (5 X 100 hr inspection)		$808,425.01
TOTAL (3 X 100 hr inspection)		$6,622,275.14
TOTAL (5 X 100 hr inspection)		$10,834,868.25

9.5. Cost Reduction

The variable that affects cost the most is the weight of the aircraft. A way in which the weight of the aircraft was minimized was by using advanced composites. Another characteristic which keeps the cost low is the quantity of aircrafts produced and the corresponding production rate. Lastly, maintenance hours per flight hour can also increase or decrease the cost. In using composite materials and state of the art technology, maintenance hours will be minimal since parts will be more accessible – unlike the F-14 which is also a variable swept aircraft but requires 50 hours of maintenance per every flight hour.

Table 9.31: Summary Totals: ***Where C_E is the airframe engineering hours, C_T is tooling, C_{ML} is labor, C_{MM} is manufacturing materials, C_{EN} is the engine(s), C_{QC} is quality control, C_D is development support, and C_P is the profit.***

C_E	$4,762,881,068
C_T	$2,553,770,592
C_{ML}	$10,427,698,469
C_{MM}	$5,079,730,292
C_{EN}	$7,270,000,000
C_{QC}	$1,538,871,173
C_D	$917,495,357
C_P	$3,007,521,444

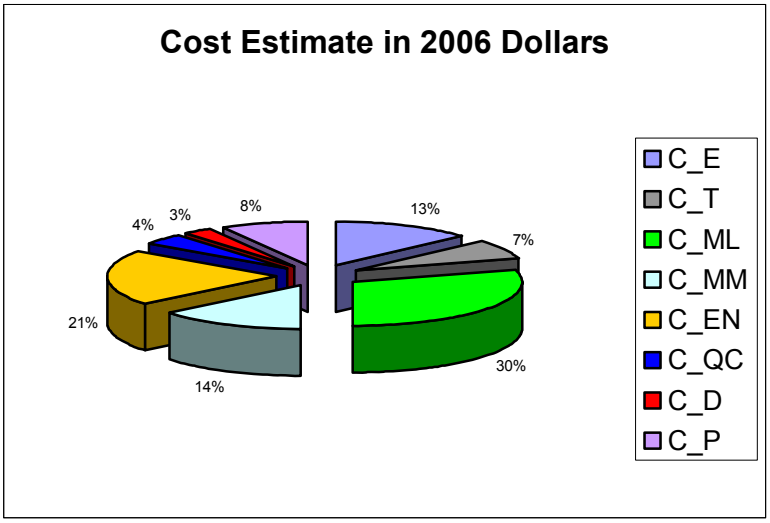

Figure 9.49: Cost breakdown ***Where C_E is the airframe engineering hours, C_T is tooling, C_{ML} is labor, C_{MM} is manufacturing materials, C_{EN} is the engine(s), C_{QC} is quality control, C_D is development support, and C_P is the profit.***

Table 9.32: Unit Cost in 2006 US Dollars

TOTAL Acquisition Cost	$26,807,243,752.61
TOTAL RDT&E cost	$6,275,492,128.93
TOTAL Flyaway Cost	$16,146,514.07
TOTAL O/M	$10,834,868.25
UNIT COST TOTAL	$53,788,626.07
	$60,064,118.20

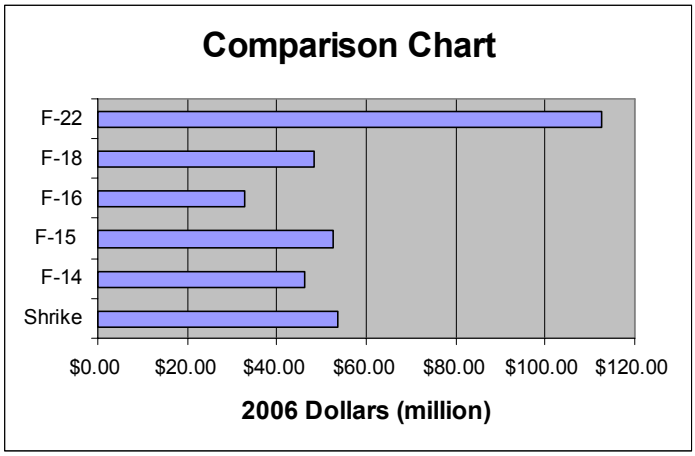

Figure 9.50: Comparing the *Shrike* to Other Fighters[33]

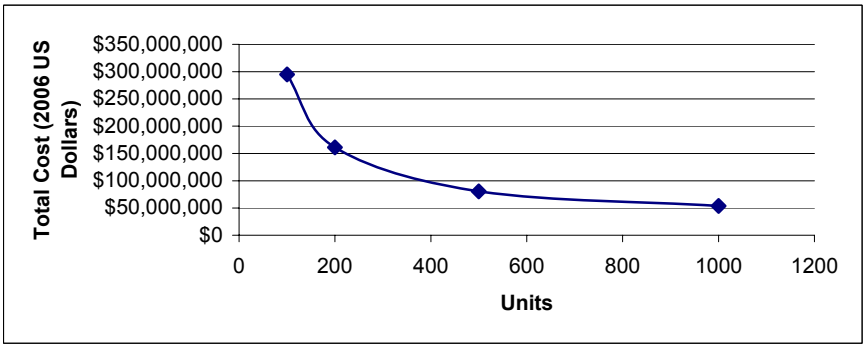

Figure 9.51: Learning curve for the total life cycle cost depending on number of units

In conclusion, as it is seen in Table 9.32, the cost of the *Shrike* per aircraft will be between $53.7 million to $60 million if 1000 units are produced. The gap in price is due to the rate of production and the manufacturing of materials as it is noted in Table 9.31. However, once the RDT&E phase is done with production the price will remain consistent and will be in the range of $53 million per aircraft since only acquisition cost is taken into account. Taking a look at Figure 9.51, it can be seen that for 100 units the total cost will be $295K and 500 units will be $80K. Looking at Figure 9.50, the *Shrike* is competitive in range with the F-15 in comparison to the F-22. It is in

a similar price range to modern fighters, with the exception of the F-22, yet having similar advanced technologies as the Raptor. Without having to take into account stealth capabilities the cost is drastically lower than the F-22.

10. Conclusion

Razerwerks Inc presents a low cost, light weight, high performance interceptor that meets or exceeds all the requirements set by the 2005-2006 AIAA Foundation Undergraduate Team Aircraft Design Competition's RFP. The *Shrike* utilizes a variable sweep wing configuration that optimizes performance at both subsonic and supersonic speeds. The 18° per second instantaneous turn rate proved to be a very influential and difficult requirement to meet; therefore, the resulting fall-out parameters, shown in Table 10.33, vastly exceed all other RFP design requirements.

Table 10.33: Conclusion of Requirements versus Capabilities: **with maximum fuel, range may be extended to 5200 nm. **Performance at Maneuver Weight (50% Internal Fuel for two AIM-120 + M61A1 gun with 500 Rounds 20mm Ammunition.*

Criteria	Requirement	*Shrike's* Capability
Intercept Radius	200 nm	200* nm
DCAP Mission Endurance	4 hrs	4 hrs
Max Mach @ 35 kft**	2.2	2.2
1-g SEP @ Max Thrust**		
0.9M/ Sea Level	200 fps	753.5 fps
0.9M/15 kft	50 fps	404.7 fps
1-g SEP @ Mil Thrust**		
0.9M/ Sea Level	700 fps	1340.6 fps
0.9M/15 kft	400 fps	825.8 fps
5-g SEP @ Max Thrust**		
0.9M/ Sea Level	300 fps	1260.3 fps
0.9M/15 kft	50 fps	691.2 fps
SLF @ Max Thrust**	5 g's	9.4 g's
Max ITR @ 35 kft**	18 deg/s	19.5 deg/s

The final advanced concept interceptor employs various advanced technologies that are both original by design and currently implemented on advanced fighters. Integration of modern techniques in structures allows for the utilization of a strong wing carry through box without raising cost or weight of the aircraft. The inclusion of advanced materials and current higher order technology allow the variably sweeping wing concept to be a cost-effective, viable solution. Thrust vectoring, coupled with differential control surfaces, aids greatly in decreasing drag and allows for greater moments leading to extreme maneuverability with smaller moving components. Fly-by-light control systems quicken data transfer throughout the aircraft while reducing weight from traditional methods.

There are significant differences in the preliminary design of the *Shrike* and the designs of the F-14 *Tomcat*. The F-14 did have similar multi-mission requirements – specifically the deck launch intercept and combat air patrol missions. The major difference lies within loiter/endurance requirements. Even if the F-14 was stripped of its bulked up airframe for carrier launches, it would still have significant issues with fuel storage for a four hour loiter followed

by an additional supersonic dash. The most the F-14 can loiter is around 2 hours with exterior fuel pods, which are not conformed to the shape, resulting in jettisoning the pods if the aircraft needs to dash at high speeds. The F-14 compensates for its tremendous fuel usage by having the ability to support mid-air refueling; however, the AIAA RFP prevents any refueling to take place during the mission, which prevents the F-14 from completing most of the design missions. The F-14 is made almost entirely of metal and has a complicated titanium wing box. Over time chance of metal fatiguing, cracking and corroding increases greatly resulting in more time, maintenance and cost of keeping the F-14 flight certified. The *Shrikes* composite structure reduces all elements of fatigue and is more cost efficient during its service life.

Upgrades and derivations of the *Shrike* have been anticipated if this design were to be produced. A reflexing flap system, similar to the F-16, and further advances in wing/tail appendages could be used in order to further increase the efficiency in all flight regimes whether take-off transition, transonic maneuvering, or supersonic dash. Airbrakes could be utilized to further increase performance in transition to subsonic flight especially during offensive intercept maneuvers. Armaments, including advances in the M-61 cannon and highly developed missile technology, could easily replace the existing weaponry issued by the RFP. Future advancements in materials manufacturing can replace panels, control surfaces, etc. and will continually become more cost-effective. The engines are easily removable resulting in an efficient maintenance improvement to the power plants.

The ability to blend modern technology along with proven techniques and applied on an efficient variable sweep design allowed for the creation of a cost effective, multi-capability interceptor to dominate the world's top threats and protect the United States of America now, and well into the future.

[1] Raymer, Daniel P. *Aircraft Design: A Conceptual Approach, Third Edition.* AIAA, Inc. 1999
[2] Abbott, Ira H. and Albert E. Von Doenhoff. *Theory of Wing Sections*. New York: Dover Publications, 1959.
[3] Brandt, Steven A. *Introduction to Aeronautics: A Design Perspective*. Reston, VA: AIAA, 2004.
[4] Mason, William H. "FRICTION". Jan. 2006. Department of Aerospace and Ocean Engineering – Virginia Tech. Feb. 2006. <http://www.aoe.vt.edu/~mason/Mason_f/MRsoft.html>
[5] "AWAVE". Jan. 2006. Department of Aerospace and Ocean Engineering – Virginia Tech. Mar. 2006. <http://www.aoe.vt.edu/~mason/Mason_f/MRsoft.html>
[6] Hepperle, Martin. "JAVAFOIL". 8 July 2004. Apr. 2006. <http://www.mh-aerotools.de/airfoils/javafoil.htm>
[7] Roskam, Dr. Jan. *Part II: Preliminary Configuration Layout and Propulsion System Integration*. Design, Analysis and Research Corporation, Lawrence, Kansas.
[8] "Software for Aerodynamics and Aircraft Design (W.H. Mason, Virginia Tech)." <http://www.aoe.vt.edu/~mason/Mason_f/MRsoft.html#ControlPower.> Last accessed on April 18, 2006
[9] Roskam, Dr. Jan. *Part VII: Determination of stability, Control and Performance Characteristics: FAR and Military.* Design, Analysis and Research Corporation, Lawrence, Kansas.
[10] Pratt & Whitney. "F100". 9 Feb. 2004. <http://www.pratt-whitney.com/prod_mil_f100.asp> <http://www.geae.com/engines/military/f110/index.html>
[11] Rolls Royce. "EJ200". Rolls Royce Defence Aerospace. <http://www.rolls-royce.com/defence_aerospace/products/combat/ej200/default.jsp>
[12] Reade Advanced Materials. 2005. <www.reade.com>
[13] "MEE433B Aluminum-Lithium Alloys". Queens University Mechanical and Materials Engineering, 2001-2005. <me.queensu.ca/courses/mech412/Notes/aluminum-lithium.doc>
[14] "Titanium Alloys". eFunda. 2005. <www.efunda.com/materials/alloys/titanium/titanium.cfm>
[15] Ashley, Steve. "Carbon Composites Fly High". The American Society of Mechanical Engineers. <www.memagazine.org/backissues/september97/features/carbon/carbon.html>
[16] MatWeb Material Property Data. 2006. <www.matweb.com>
[17] "High Speed Research – F22 Raptor". All Star Network. 12 Mar. 2004. <www.allstar.fiu.edu/aero/f22raptor.html>
[18] Nipper, Mike. "LOCKHEED MARTIN DEMONSTRATES RESIN TRANSFER MOLDING TECHNOLOGY IN ADVANCED FIGHTER VERTICAL TAIL PROJECT". Lockheed Corporation. 2005. <http://www.lockheedmartin.com/wms/findPage.do?dsp=fec&ci=15651&rsbci=0&fti=112&ti=0&sc=400>
[19] Niu, Michael C.Y. *Airframe Structural Design.* Conmilit Press Inc, 1988. Burbank, California.
[20] Inventor Professional version 10. Autodesk, Inc. March, 18, 2005
[21] Nelson, Bud D. "Design Scope for Student Supersonic Projects." 1987
[22] Kreisher, Otto. "Unmanned Combat Planes are 'smarter'…" Military.com
[23] Botten, Stephen L. Whittley, King. "Flight Control Technology…" Technology Review Journal. Fall/Winter 2000
[24] Dermis, Thomas F., Joseph P. Nalepka, Daniel B Thompson, et. al. Air Force Research Laboratory. <http://www.afrlhorizons.com/Briefs/Apr05/VA0412.html>
[25] "FADEC." March 2006. <http://en.wikipedia.org/FADEC>
[26] "Joint Strike Fighter." May 2006. <http://www.jsf.mil/f35/f35_technology.htm>
[27] "Thermion systems." <http://www.emerald-library.com/Insight/>
[28] "Semi-submerged Missiles." <http://www.ejectionsite.com/F-14_20SHOOTDOWN.pdf>
[29] "AMRAAM Missiles." <http://en.wikipedia.org/wiki/AMRAAM>
[30] Roskam, Dr. Jan. *Airplane Design, Part VIII: Airplane Cost Estimation*. University of Kansas. 1990.
[31] Corke, Thomas. *Design of Aircraft.* New York: Prentice Hall, 2002.
[32] "CPI Inflation Calculator". U.S. Department of Labor. March 2006. < http://data.bls.gov/cgi-bin/cpicalc.pl>
[33] U.S. Military Aircraft. Federation of American Scientists. Military Analysis Network. April 2006. <http://www.fas.org/man/dod-101/sys/ac/>